NAVAL POSTGRADUATE SCHOOL
Monterey, California

THESIS

EXAMINATION OF THE 13 FEBRUARY 2001 EASTERN PACIFIC MARITIME CYCLOGENESIS

by

Marc E. Touchton

March 2002

Thesis Advisor:	Wendell A. Nuss
Second Reader:	Douglas K. Miller

Approved for public release; distribution is unlimited.

THIS PAGE INTENTIONALLY LEFT BLANK

REPORT DOCUMENTATION PAGE			Form Approved OMB No. 0704-0188
Public reporting burden for this collection of information is estimated to average 1 hour per response, including the time for reviewing instruction, searching existing data sources, gathering and maintaining the data needed, and completing and reviewing the collection of information. Send comments regarding this burden estimate or any other aspect of this collection of information, including suggestions for reducing this burden, to Washington headquarters Services, Directorate for Information Operations and Reports, 1215 Jefferson Davis Highway, Suite 1204, Arlington, VA 22202-4302, and to the Office of Management and Budget, Paperwork Reduction Project (0704-0188) Washington DC 20503.			
1. AGENCY USE ONLY ***(Leave blank)***	**2. REPORT DATE** March 2002	**3. REPORT TYPE AND DATES COVERED** Master's Thesis	
4. TITLE AND SUBTITLE: Examination of the 13 February 2001 Eastern Pacific Maritime Cyclogenesis			**5. FUNDING NUMBERS**
6. AUTHOR(S) Marc E. Touchton			
7. PERFORMING ORGANIZATION NAME(S) AND ADDRESS(ES) Naval Postgraduate School Monterey, CA 93943-5000			**8. PERFORMING ORGANIZATION REPORT NUMBER**
9. SPONSORING /MONITORING AGENCY NAME(S) AND ADDRESS(ES) N/A			**10. SPONSORING/MONITORING AGENCY REPORT NUMBER**
11. SUPPLEMENTARY NOTES The views expressed in this thesis are those of the author and do not reflect the official policy or position of the Department of Defense or the U.S. Government.			
12a. DISTRIBUTION / AVAILABILITY STATEMENT Approved for public release; distribution is unlimited.			**12b. DISTRIBUTION CODE**

13. ABSTRACT ***(maximum 200 words)***

On 13 February 2001, an explosive cyclone made landfall in Southern California. This system was responsible for storm force winds and heavy precipitation in the Los Angeles area. This storm is interesting because it was handled poorly by the numerical models and developed in an unusual area.

Analysis of this storm revealed double circulation centers and multiple baroclinic zones. Due to weak static stability, air-sea fluxes were contributory in developing the baroclinic zone from which this cyclone originated as well as enhancing its development rate. Evidence suggests that the system may have had a warm core, similar to other intense extratropical cyclones.

The models did not properly forecast this system due to weak cold air advection over the Eastern Pacific Ocean and due to blending the subpolar and subtropical jets into a single feature. Data assimilation is suspected to have played a role in the mishandling of these key features.

14. SUBJECT TERMS Explosive Cyclogenesis, Maritime Cyclogenesis, NOGAPS, COAMPS, Air-Sea Fluxes			**15. NUMBER OF PAGES** 63
			16. PRICE CODE
17. SECURITY CLASSIFICATION OF REPORT Unclassified	**18. SECURITY CLASSIFICATION OF THIS PAGE** Unclassified	**19. SECURITY CLASSIFICATION OF ABSTRACT** Unclassified	**20. LIMITATION OF ABSTRACT** UL

NSN 7540-01-280-5500

Standard Form 298 (Rev. 2-89)
Prescribed by ANSI Std. 239-18

THIS PAGE INTENTIONALLY LEFT BLANK

Approved for public release; distribution is unlimited.

EXAMINATION OF THE 13 FEBRUARY 2001 EASTERN PACIFIC MARITIME CYCLOGENESIS

Marc E. Touchton
Lieutenant Commander, United States Navy
B.A., Memphis State University, 1991

Submitted in partial fulfillment of the
requirements for the degree of

MASTER OF SCIENCE IN METEROLOGY AND PHYSICAL OCEANOGRAPHY

from the

NAVAL POSTGRADAUTE SCHOOL
March 2002

Author: Marc E. Touchton

Approved by: Wendell A. Nuss
Thesis Advisor

Douglas K. Miller
Second Reader

Carlyle H. Wash
Chairman, Department of Meteorology

THIS PAGE INTENTIONALLY LEFT BLANK

ABSTRACT

On 13 February 2001, an explosive cyclone made landfall in Southern California. This system was responsible for storm force winds and heavy precipitation in the Los Angeles area. This storm is interesting because it was handled poorly by the numerical models and developed in an unusual area.

Analysis of this storm revealed double circulation centers and multiple baroclinic zones. Due to weak static stability, air-sea fluxes were contributory in developing the baroclinic zone from which this cyclone originated as well as enhancing its development rate. Evidence suggests that the system may have had a warm core, similar to other intense extratropical cyclones.

The models did not properly forecast this system due to weak cold air advection over the Eastern Pacific Ocean and due to blending the subpolar and subtropical jets into a single feature. Data assimilation is suspected to have played a role in the mishandling of these key features.

THIS PAGE INTENTIONALLY LEFT BLANK

TABLE OF CONTENTS

LIST OF FIGURES

LIST OF TABLES

THIS PAGE INTENTIONALLY LEFT BLANK

ACKNOWLEDGMENTS

The author would like to thank the following individuals for their support of this thesis:

Prof. Nuss for your support and guidance as thesis advisor.

Prof. Miller for your direction as second reader.

Mr. Bob Creasey for your indispensable technical support and tireless efforts with data display and collection.

THIS PAGE INTENTIONALLY LEFT BLANK

I. INTRODUCTION

On 12 and 13 February 2001, an explosively deepening cyclone came on shore in Southern California. This system was responsible for up to 5 inches of rain and storm force winds in some areas. In spite of substantial advances in numerical weather prediction (NWP) in recent years, this storm, which impacted a large metropolitan area, was poorly handled in numerical forecasts. The development of this storm in an unusual area further increased its impact on Southern California.

The sea level pressure (SLP) trend, which is based on a hand analysis performed for this storm, is shown in Figure 1.1. From 2000 UTC 12 February to 0600 UTC 13 February (date/time information will hereafter be abbreviated as 12/20 and 13/06, etc.), the storm experienced mild cyclogenesis with a deepening rate of about 1 mb/hr. Over the next 6 hours, the storm deepened rapidly at a rate of 2 mb/hr. After 13/12, the maximum intensity for the storm, the cyclone weakened and began to fill as it moved on shore.

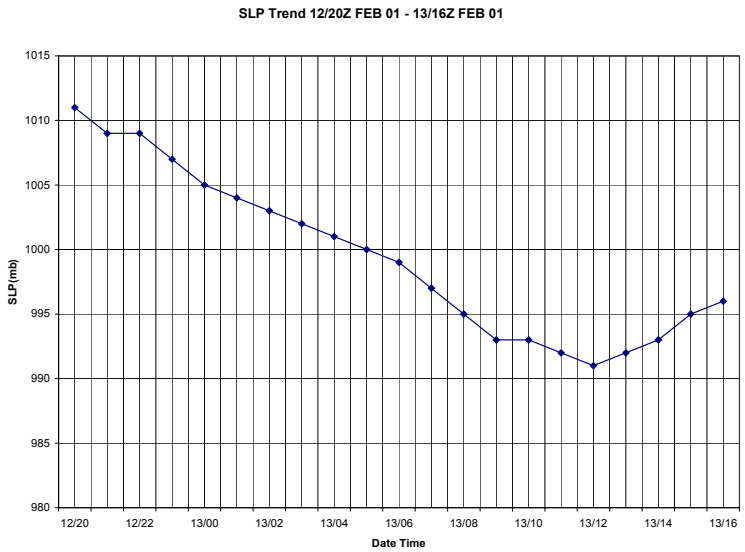

Figure 1.1 Sea level pressure trend of the storm based on the hand analysis.

Numerical model forecasts had a difficult time in the initial development of this storm and its rapid deepening. In general, the 24-hour model forecasts performed better than the 12-hour forecasts. Of particular note, the Navy Operational Global Atmospheric

Prediction System (NOGAPS) and the Coupled Ocean and Atmosphere Mesoscale Prediction System (COAMPS) forecast runs from 12/12 February failed to depict this cyclone until the 24-hour forecast. Not readily obvious from the model fields is why this cyclone developed at all. The purpose of this thesis is to investigate the driving factors in the development of this storm, to examine why the NWP guidance was poor and to provide greater understanding of maritime cyclogenesis.

The emphasis in this study was to document the detailed evolution of this storm in order to describe the dynamical processes that lead to its rapid development. From this groundwork, the critical elements that the models missed that were necessary to accurately forecast this system could be identified. The upper level dynamic support, as well as air-sea fluxes, were examined to determine their potential role in the development of this system. Finally, this case study will add to and amplify the current understanding of maritime cyclogenesis through comparison to other cyclones.

Beneficial to the efforts of this thesis was that the Pacific Landfalling Jets Experiment (PACJET) 2001 Study coincided with the timeframe of the cyclone. PACJET 2001 provided additional data through an aircraft flight and dropsondes that would have otherwise been unavailable. These PACJET observations were used in conjuction with other data sources to provide a more complete description of the evolution of this cyclone.

This thesis begins by reviewing the factors important to maritime cyclogenesis. Chapter III then provides a synoptic description of the cyclone based on surface observations and other related data. The performance of the operational models will be covered in Chapter IV. The computation and impact of air-sea fluxes on this storm are discussed in Chapter V. The thesis will conclude with the findings and conclusions in Chapter VI.

II. IMPORTANT ASPECTS OF MARITIME CYCLOGENESIS

The goal of this chapter is to provide a background into the important aspects of cyclogenesis, with an emphasis on maritime characteristics. The first two sections will discuss accepted theories on cyclogenesis. The final section will point out differences unique to this system that do not fit the general theories.

A. METEOROLOGICAL DYNAMICS

1. Petterssen Development Theory

As described by Djurić (1994), Petterssen's development theory considered two types of cyclone development, Type A and B. In Type A development, the upper level flow is essentially straight. Warm and cold advection at the surface creates an upper-level ridge and trough, respectively. This type is described as an amplifying frontal wave. Type B development involves a pre-existing upper-level trough that interacts with a surface baroclinic zone. The development of the surface cyclone through interaction with the upper level trough is due to vorticity advection and jet diffluence.

2. Vorticity Advection

Positive vorticity exists in the cyclonic turning at the base of an upper level trough, which results in negative/positive vorticity advection on the upstream/downstream side of the trough. A surface system under the downstream side of the trough is favorable for cyclogenesis. This places the system in the region of positive vorticity advection (PVA) and coupled to surface convergence that allows the system to deepen. The magnitude of the vorticity advection is determined in part by the magnitude of the flow and the magnitude of the vorticity maximum. A narrower trough with higher winds will produce higher PVA than a broader trough with lower winds. Rapid cyclogenesis is often associated with a stronger trough that produces large PVA aloft.

3. Jets

As noted by Uccellini (1990) and others, jet streaks can play a significant role in cyclogenesis. Based upon the four-quadrant model of jet streak dynamics, the right entrance region and the left exit region of jet streaks are divergent with the opposite regions being convergent. When a low level baroclinic zone or low pressure system are

positioned under the divergent regions of the jet streak, upward vertical motion occurs over the surface feature. This vertical motion allows for the reduction of pressure and convergence at the surface, which contribute to the amplification of the surface system.

B. AIR-SEA FLUXES

Nuss (1989), using an idealized maritime cyclone, modeled the influence of air-sea fluxes on its development. Differing effects were found depending upon the static stability of the atmosphere and where the upward fluxes occurred in relation to the storm center.

If the upward fluxes were collocated with the cyclone and the atmosphere was statically stable, the fluxes hindered cyclogenesis. If, however, the atmosphere were statically unstable, the upward fluxes would have a positive contribution to cyclogenesis. This effect is due to the ability of the upward fluxes to mix vertically to the upper atmosphere and alter the upper level dynamics.

The second favorable combination occurs when the upward fluxes were located to the northeast of the developing storm. This allowed the fluxes to add heat and moisture to the air ahead of the warm front which would then contribute more moisture to release as latent heat and thereby enhance cyclogenesis. A necessary condition for this case to occur was the preconditioning of the region by an outbreak of cold air, as in behind a recent preceding cold front.

C. DIFFERENCES UNIQUE TO THIS SYSTEM

1. Pre-existing Baroclinic Zone

The generally accepted theory requires an existing surface baroclinic zone to interact with a propagating upper level trough for cyclogenesis to occur (polar front theory). Given this condition, the most likely areas for cyclogenesis are along existing frontal features, either from an extratropical cyclone or a coastal front associated with a western boundary current such as the Gulf Stream.

This cyclone, however, did not develop from a pre-existing baroclinic zone. The development of this baroclinic zone will be discussed in Chapter V. The development region for this cyclone was over the open ocean which had recently experienced the

passage of a cold front. The air mass was characteristically cold with weak horizontal thermal gradients and low static stability.

2. Unfavorable Development Region

Roebber (1984) completed a statistical and climatological study on explosive cyclones. Using the "Bergeron" definition for explosive cyclogenesis, Roebber (1984) determined the lower limit of 24-hour pressure falls to be 19 mb for a cyclone to considered explosive. Applying this limit, Figure 2.1 shows the distribution of formation positions for explosive cyclones in a one-year sample. The majority of the Pacific Ocean and especially the Eastern Pacific are not historically favorable for explosive cyclogenesis. This is due to the characteristically cold waters forming a nearly uniform air mass with weak surface baroclinicity. The upper level troughs are generally decaying and have weak PVA in this area.

However, cyclones do develop in this region, which represents a combination of factors that differ from the mean. This study examines these factors as they pertain to this case.

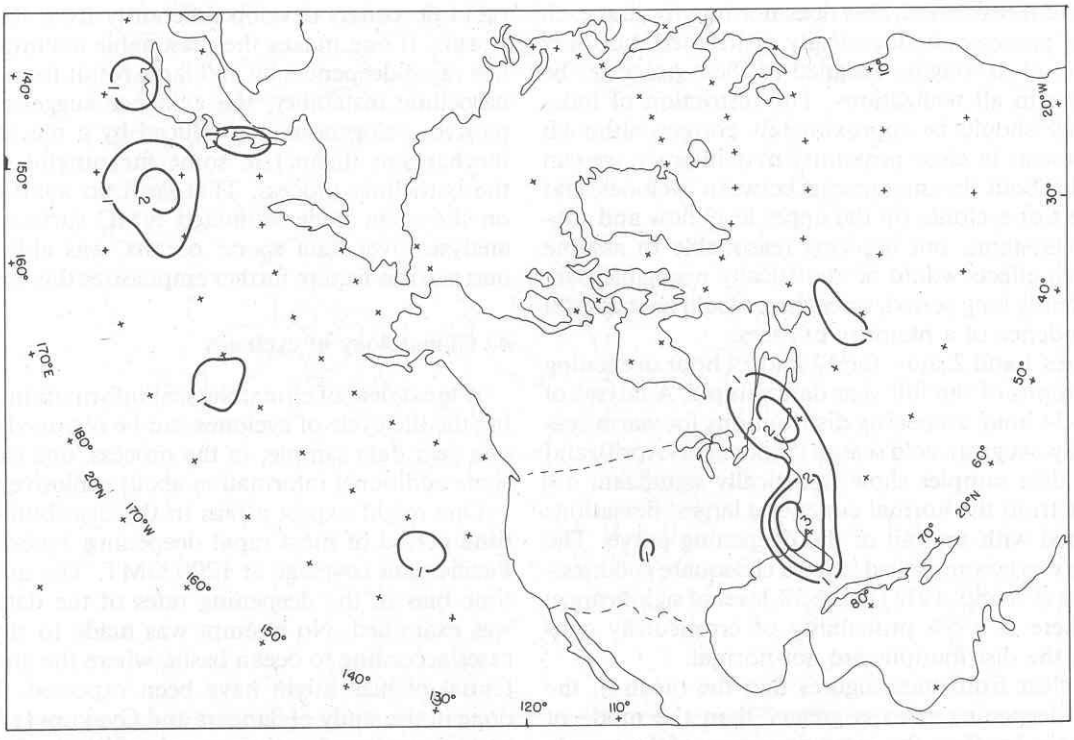

Figure 2.1. Distribution of formation positions for explosive cyclones from February 1980 to January 1981. (from: Roebber, 1984)

THIS PAGE INTENTIONALLY LEFT BLANK

III. 12-13 FEBRUARY CYCLONE ANALYSIS

This chapter provides a synoptic description of the evolution of the cyclone based upon a hand analysis of the surface observational data and of the upper level dynamic support structure. First a description of the analysis procedures will be detailed. Then, the synoptic description of the 500-mb dynamic structure and surface pressure will be discussed.

A. ANALYSIS METHOD

A hand analysis was performed to obtain a better understanding of the evolution of this unique system. The surface pressure analysis was performed on an hourly basis, utilizing all available surface station observations, ship reports and buoy observations. Hourly GOES-10 infrared (IR) and visible imagery were utilized for the positioning of the system and its features. Appropriate scatterometer wind observations (SCATWIND) from satellite passes within 15 minutes of the synoptic reports and data from the PACJET 2001 aircraft also supplemented the analysis.

The upper level analysis was accomplished by overlaying satellite feature-tracked winds (SATWINDS) data within two hours of the appropriate NOGAPS analysis and GOES-10 satellite image. From these overlays, it appeared the models did not properly depict the upper level structure and that the 500 mb jet structure was better defined than above 500 mb. Figure 3.1 shows the 13/00 IR satellite image with NOGAPS 500 mb isotachs in knots overlaid. In the bottom of the image, the high clouds associated with the subtropical jet can be seen moving across Mexico into the southeastern United States. Also evident from the upper level clouds extending from Southern California into Nevada is the outflow of a subpolar jet streak. The NOGAPS analysis, however, has blended the two jet features into one jet positioned in between the two.

While all the models did not correctly determine the upper level structure (not shown), COAMPS 500 mb winds did the best on the intensity of the wind maxima. For this reason, the SATWINDS within two hours of the COAMPS 500 mb analysis were overlaid and streamlines were drawn to match the SATWINDS data. The COAMPS wind structure was then propagated along the analyzed structure to correspond with the

available data. This was done to achieve a more accurate depiction of the upper-level features. This resulted in two jet features, the subtropical jet well to the south and the subpolar jet crossing just over the low as consistent with the clouds in Figure 3.1.

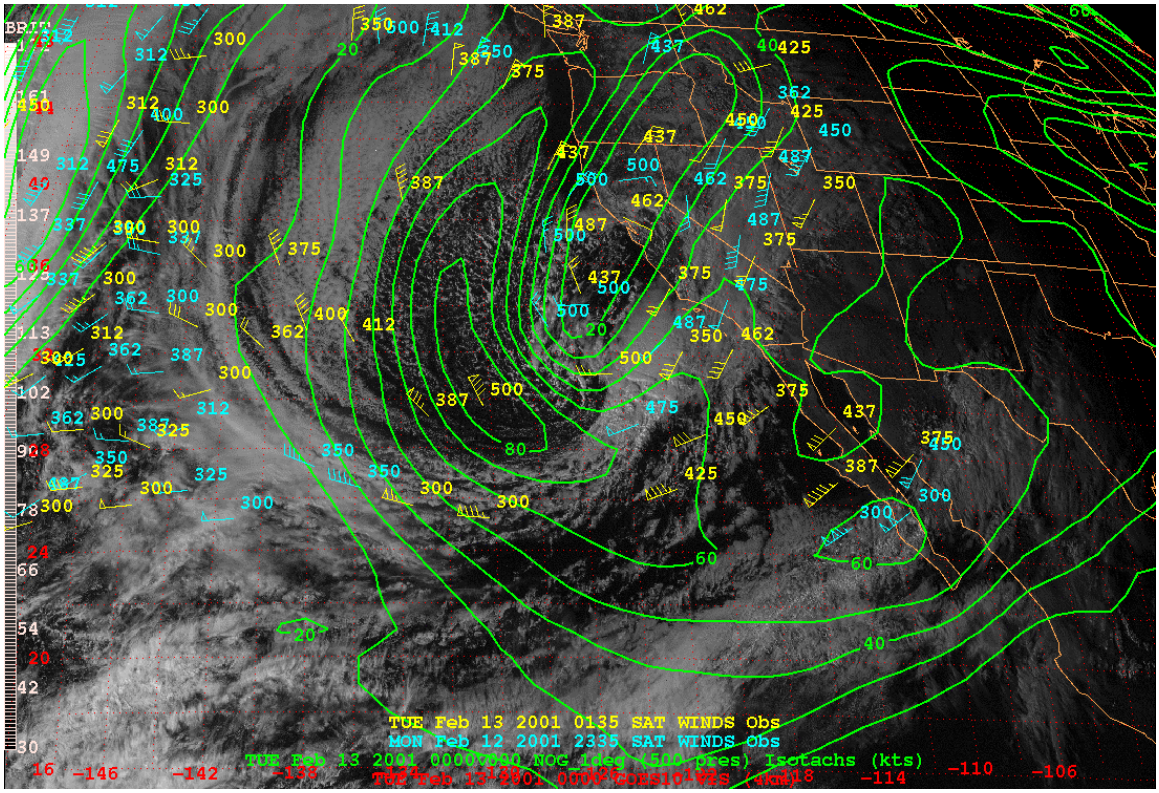

Figure 3.1. 13/00 visible satellite imagery with NOGAPS analysis of 500 mb isotachs (kt) and SATWINDS from 300 to 500 mb for 12/23 (blue) and 13/01 (yellow).

B. SYNOPTIC DESCRIPTION

The synoptic description of the structure of the atmosphere from the upper levels to the surface is described for the critical time period of this cyclone. The storm will be divided into phases as follows: 12/12 to 12/20, pre-cyclogenesis; 12/20 to 13/06, cyclogenesis; and 13/06 to 13/12, explosive deepening, which are based on the SLP trend shown in Figure 1.1. Based on the upper level analysis, the 300 mb jet structure was not found to be critical to the development of this cyclone and the 500 mb jet structure was in a more favorable position to aid the cyclogenesis. Therefore, the 500 mb level is used to characterize the upper level evolution. However, thermal advection above 500 mb may have been a key element in the development of this cyclone but was not examined in this study.

1. Synoptic Overview

By 12/06 February, the cold front associated with a low sitting over the Western United States had brought cold polar air over the Eastern Pacific Ocean. At 12/12, a region of organized convective clouds formed in the cold air mass from 32N 128W to 33 N 134 W and began to propagate to the east (Fig. 3.2a). This band of clouds rotated to a northeast to southwest orientation from 33N 124.5W to 30N 134W and began to take on a baroclinic leaf structure by 12/18 (Fig. 3.2b). This storm quickly developed a large cloud mass at 33N 123W, as shown in Figure 3.2c and slowly moved to the east. At this time, the system appears to have two baroclinic zones extending to the south. By 13/06, the trailing baroclinic zone has weakened and the storm appears as a classic extratropical cyclone in the satellite imagery at 33N 121W (Fig. 3.2d). From 13/06 to 13/12, the low explosively deepens and moves to the northeast. At 13/12, the low is located in the Channel Islands off the Southern California coast and has the appearance of an occluded low that has reached its maximum intensity (Fig. 3.2e).

2. Pre-cyclogenesis Phase

a. 500 MB

Figure 3.3 shows the 12/12 COAMPS 500 mb isotach analysis in knots overlaid on the 12/12 IR satellite image with 12/16 SATWINDS. 12/16 SATWINDS are used because earlier data that would better correspond was not available. The 500 mb pattern indicates a broad upper-level trough over the Eastern Pacific. The band of low clouds at the bottom of Figure 3.3 is located near an area of PVA, as suggested by the cyclonic turning of the winds in that region. The jet streaks are not properly located based on the SATWINDS. The 12/16 SATWINDS, despite the time difference, and the 12/12 water vapor image (not shown) suggest that the COAMPS wind maxima are too far to the west. This suggests that the 90 kt jet maxima should be located approximately 240 nautical miles to the ESE. This would place the enhanced clouds in an unfavorable position; however, as they propagate to the east the positioning will become more favorable.

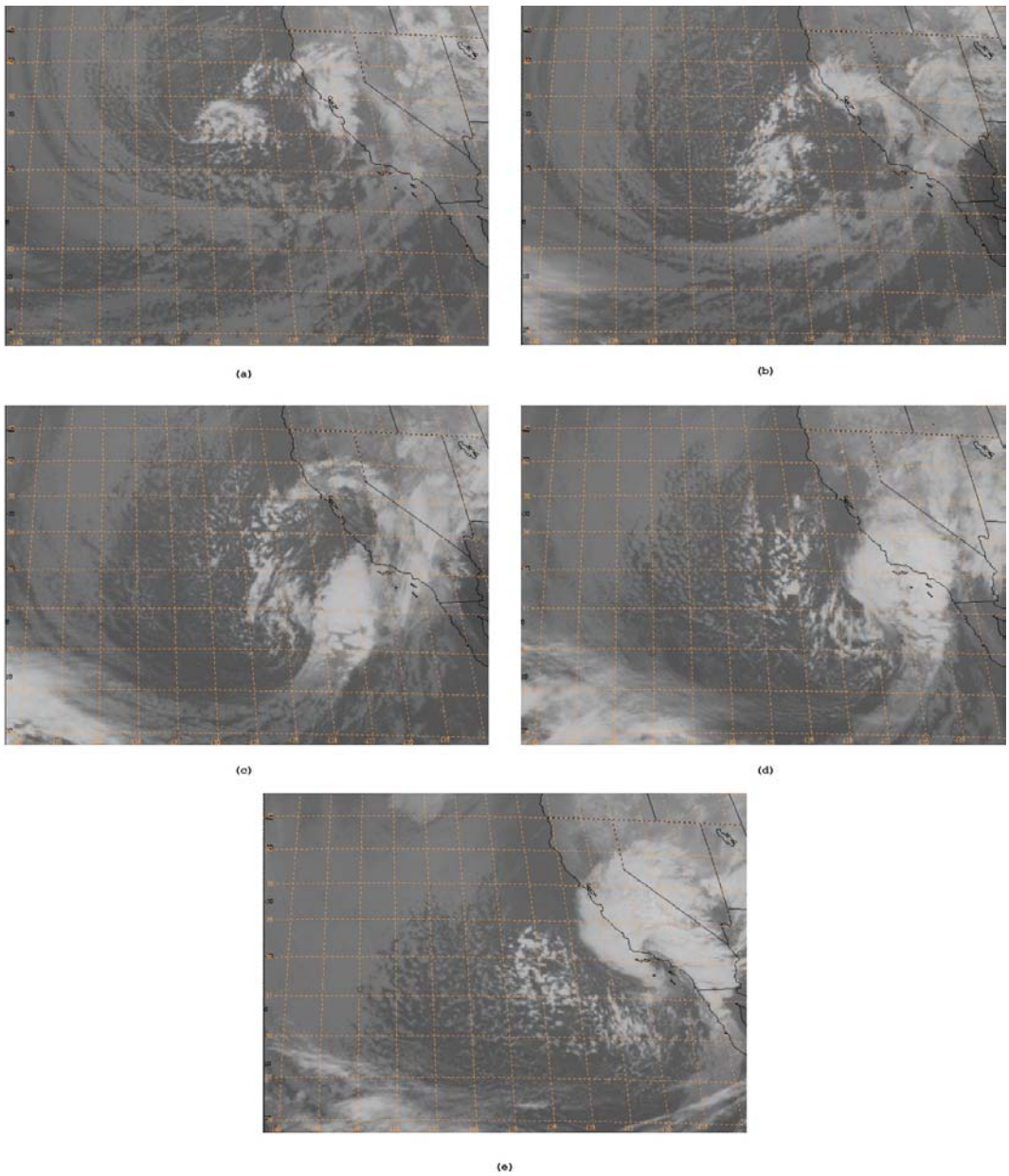

Figure 3.2. GOES-10 IR satellite imagery for (a) 12/12 February, (b) 12/18 February, (c) 13/00 February, (d) 13/06 February and (e) 13/12 February.

b. Surface

The surface analysis in Figure 3.4 shows a 1009 MB low located over north central Nevada with a cold front extending to the south then curving to the southwest across California, just south of Pt. Conception. In the cold air behind this front, a 1005 MB low sits just north of the San Francisco Bay, below the 500 mb trough center, with a small baroclinic zone extending to the south through Monterey Bay. A

baroclinic zone, determined from ship and buoy observations, has formed at 32 N 128 W and extends to the WNW to 33N 134 W and corresponds to the band of clouds in Figure 3.2a. This baroclinic zone slowly propagates to the east and begins to rotate to a northeast to southwest orientation by 12/18.

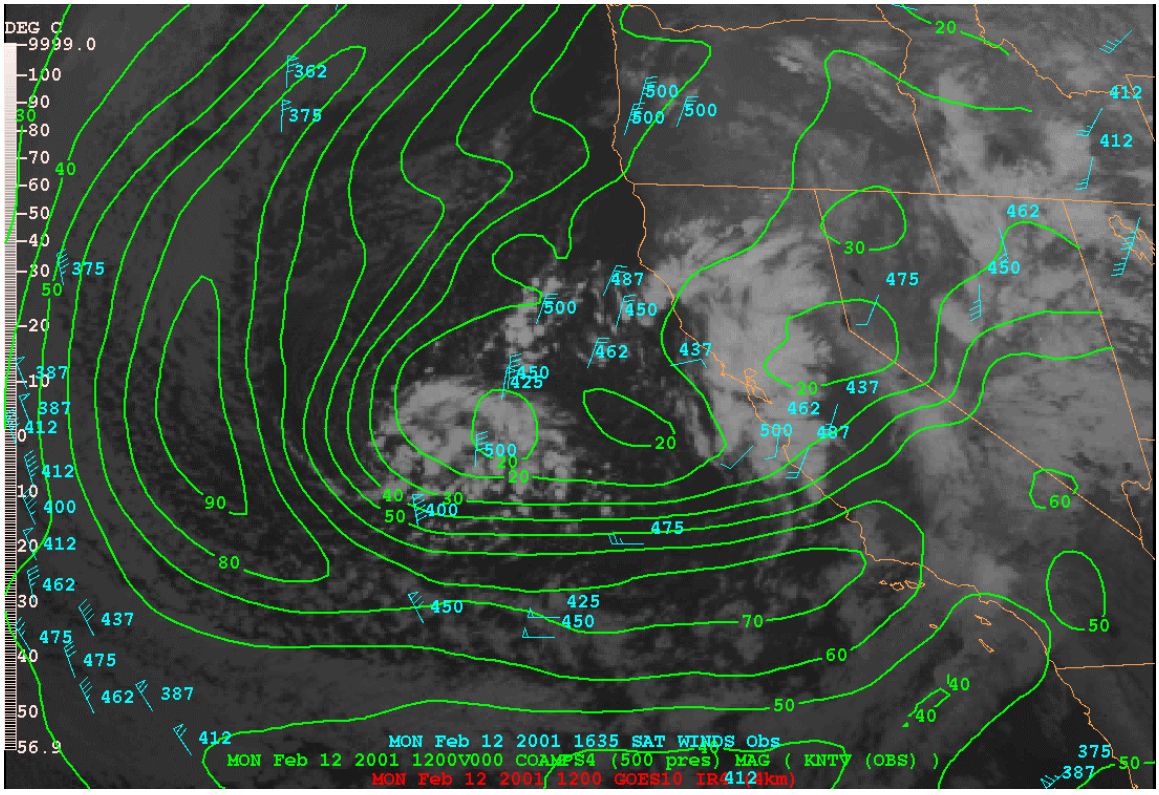

Figure 3.3. 12/12 IR satellite image with 12/12 COAMPS 500 mb isotach (kt) analysis, 12/16 300 to 500 mb SATWINDS.

Over the next 6 hours, the surface analysis in Figure 3.5 shows the Nevada low and its front have continued moving east and are essentially out of the area. The low over northern California has moved over the SF bay and has weakened and is at 1011mb. The baroclinic zone has moved to the east to about 33 N 124 W and takes on a baroclinic leaf structure in the IR imagery (Fig 3.2b). The region of enhanced convection, associated with the jet has also moved to a position just upstream of the baroclinic leaf. This suggests that the upper levels are beginning to interact with the lower levels and the cloud mass begins to grow in size and two frontal features appear to have developed by 12/19, extending from the cloud mass from 30N 122W to 28N 124W and from 30N 124W to 28N 126W (Fig. 3.6).

3. Cyclogenesis Phase

a. 500 MB

Figure 3.6 shows the 13/00 IR satellite image with the COAMPS 13/00 500 mb isotach analysis and the 12/23 and 13/01 300-500 mb SATWINDS overlaid. The SATWINDS data suggests the 500 mb trough axis is to the west of the low complex and therefore indicates a large area of PVA directly over the system. The 100 kt jet streak is located well to the west of the low in the figure. The SATWINDS indicate the jet streak should be shifted 480 nm to the ESE and rotated to an east-west orientation. Additionally, Figure 3.7 shows the 13/0159 dropsonde launched from the PACJET P-3, which indicates 90 kt at approximately 430 mb. This would place the low under the left exit region of the jet streak.

b. Surface

By 12/20 a definite low pressure system has developed with a central pressure of 1011 mb, and two circulation centers, each with a respective cold front, are suggested by imagery and observations. This dual low and frontal structure is still evident by 13/00 as shown in Figure 3.8 and will be documented more completely below. By 13/00 coastal stations in the area of Point Conception begin to show pressure falls as the system nears the coast. By 12/23, the system has a large cloud shield (Fig. 3.2c) and has become the dominant system for the eastern Pacific and reaches 1005 mb at 13/00. Behind the system the open-cell cumulus associated with the cold sector of cyclone cover the remainder of the eastern Pacific.

A 13/0114 February scatterometer pass supports the elongated pressure pattern with double circulation centers as analyzed in the surface data. The scatterometer winds were quality checked during the initial processing and should have most first order errors corrected so rain contamination would have little effect on the data displayed. Figure 3.9 shows the scatterometer pass overlaid on the 13/01 IR satellite imagery. Not exactly co-located with the cloud signature, the scatterometer winds do show two circulation centers and two lines of horizontal wind shear associated with two baroclinic zones, which are also supported by the IR satellite imagery (Fig 3.2c).

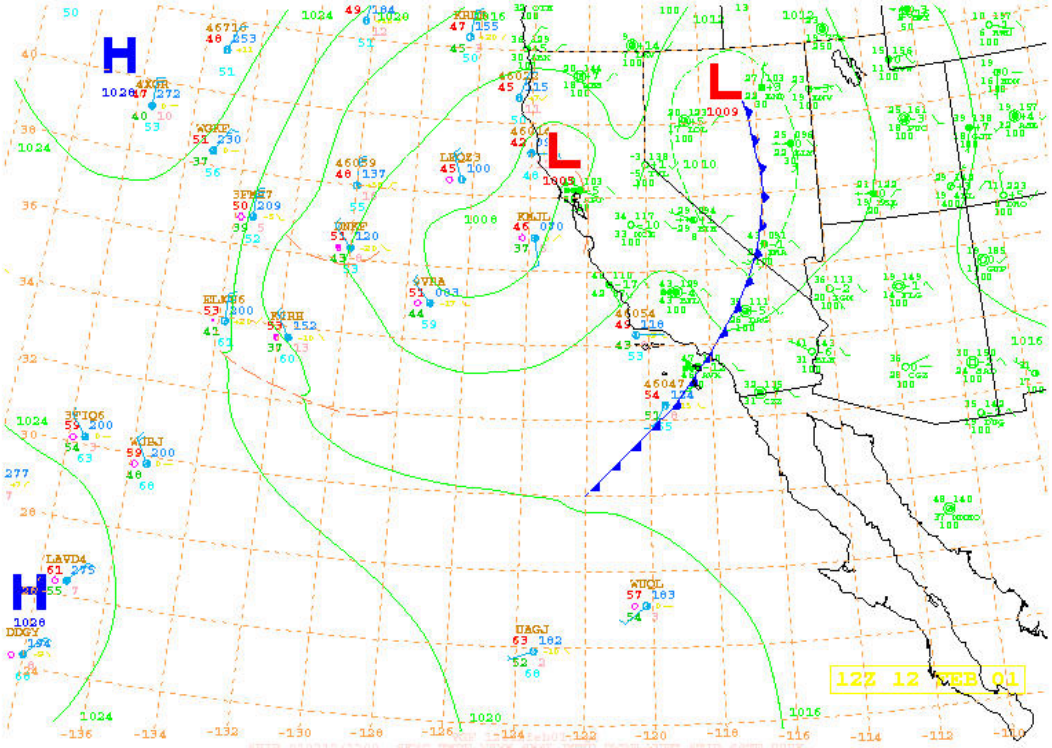

Figure 3.4. 12/12 February surface analysis with some observations plotted.

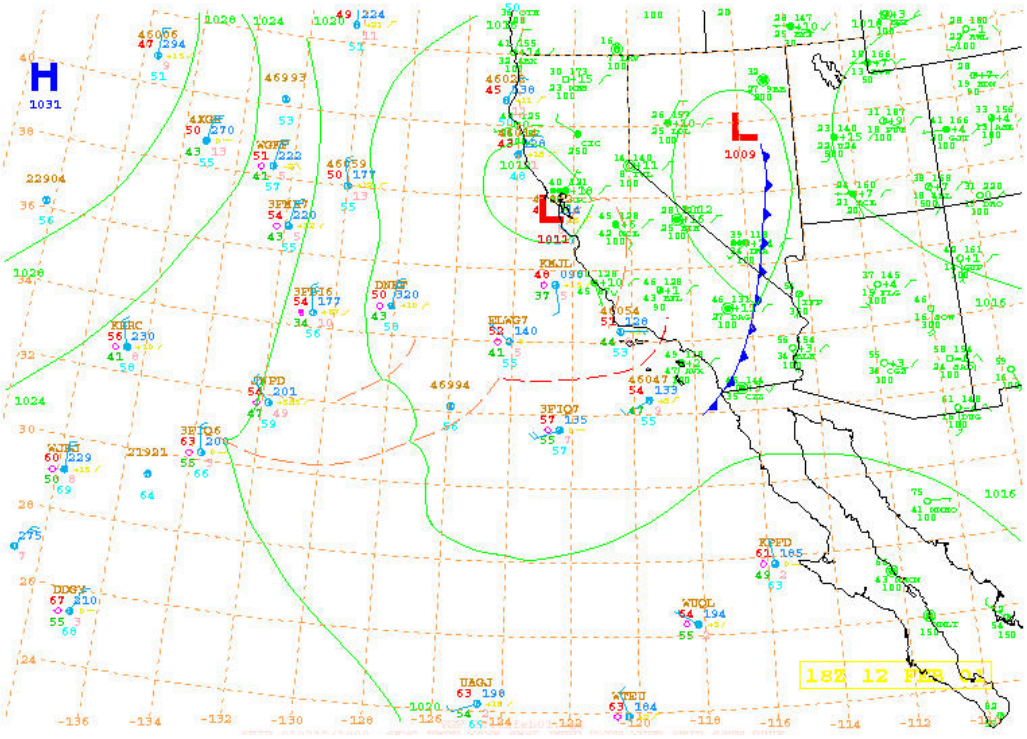

Figure 3.5. 12/18 February surface analysis with some observations plotted.

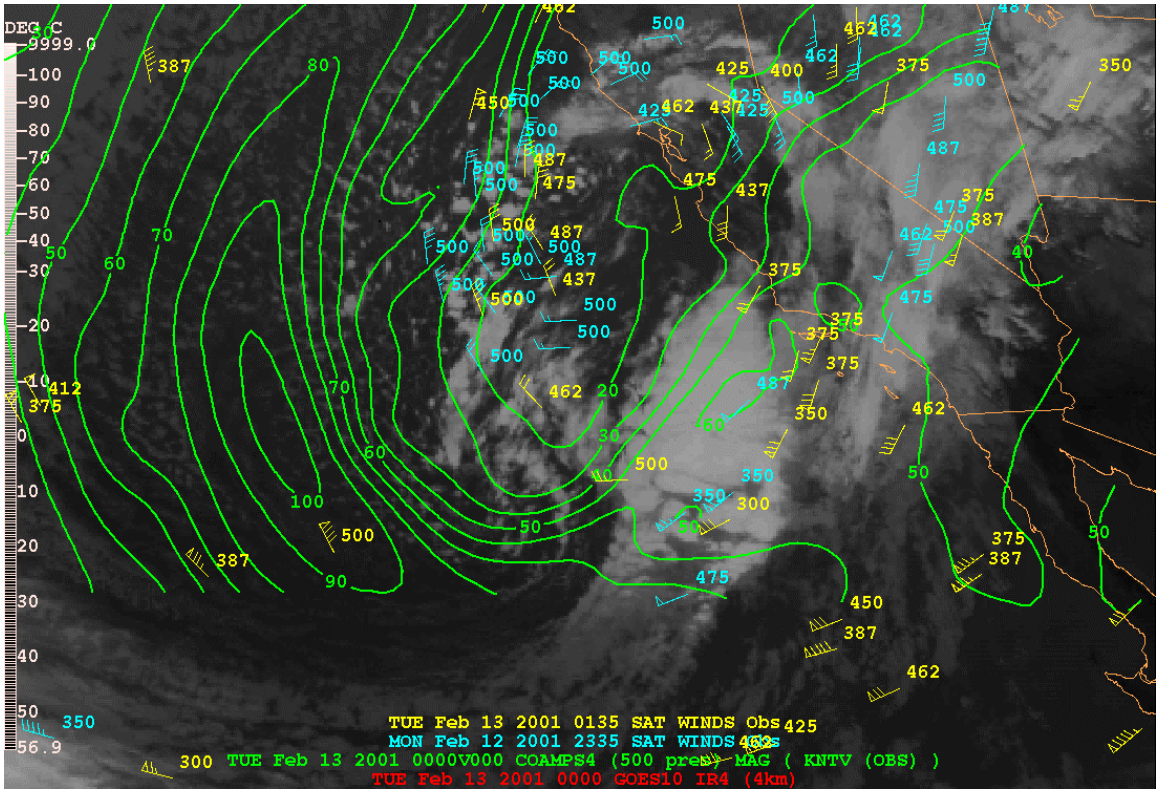

Figure 3.6. 13/00 IR satellite image with COAMPS 13/00 500 mb isotachs (kt) analysis and 300 to 500 mb SATWINDS for 12/23 (blue) and 13/01 (yellow).

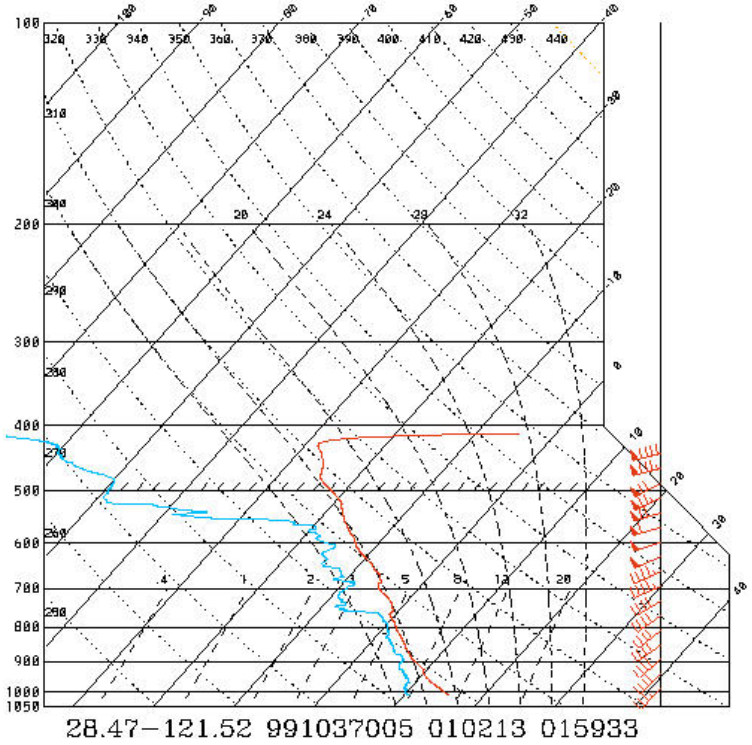

Figure 3.7. PACJET dropsonde vertical profile launched at 13/0159, 28.47N 121.52W.

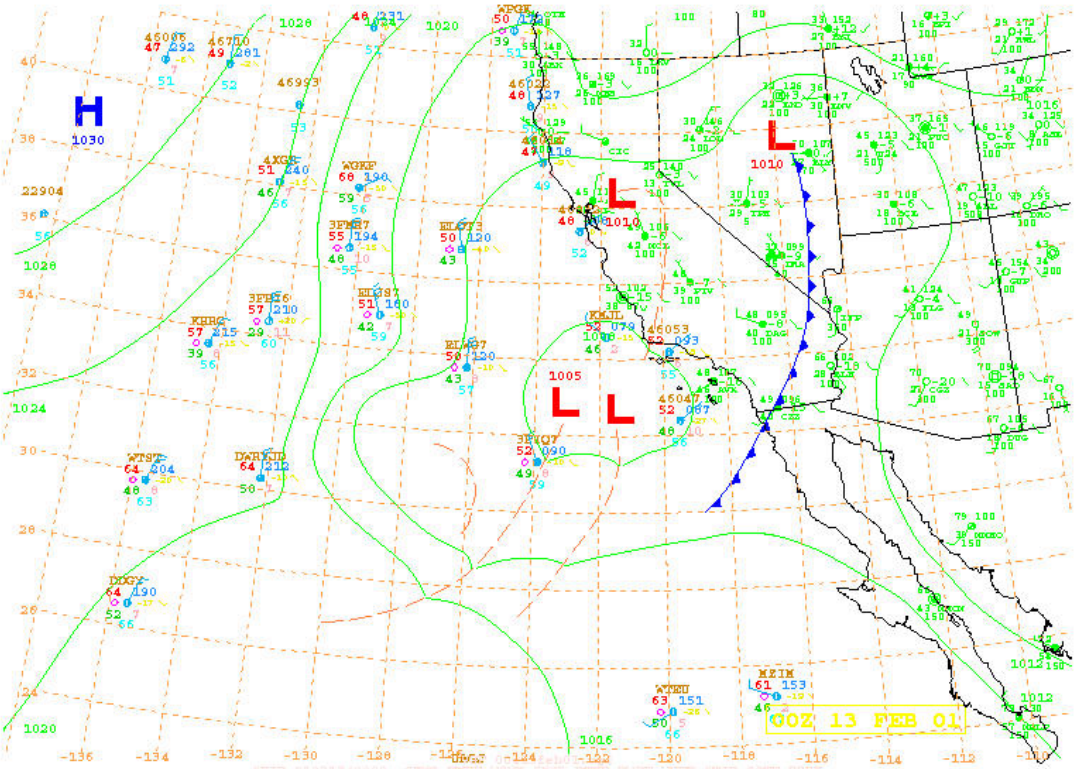

Figure 3.8. 13/00 February surface analysis with some observations plotted.

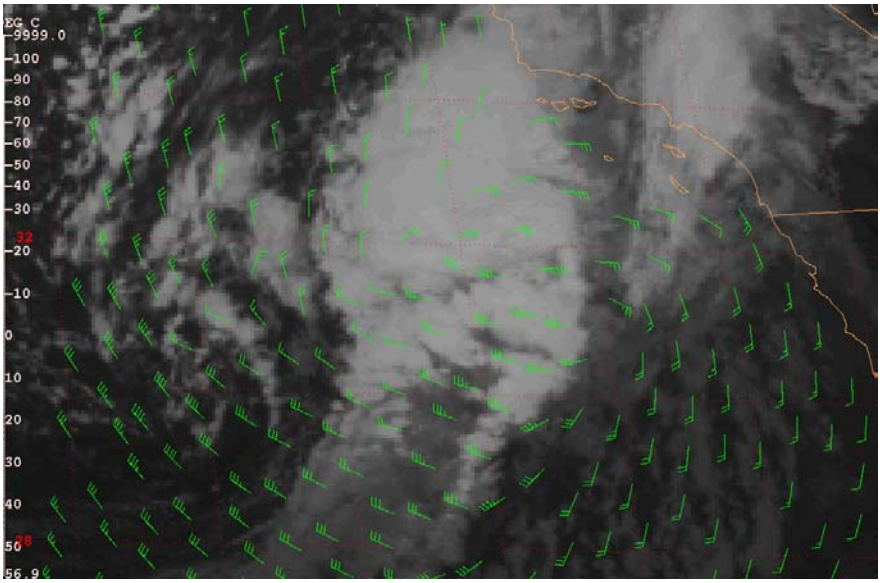

Figure 3.9. 13/01 IR satellite image with 13/0114 scatterometer winds.

Furthermore, data obtained from the PACJET 2001 P-3 aircraft support the double centers and frontal zones analyzed for this low. Dropsondes deployed from the aircraft as it traveled to the west of the storm show frontal characteristics in their temperature and wind profiles. Figure 3.10 shows the location and times of the

dropsonde launches. The 13/0100 dropsonde is shown in Figure 3.11. The temperature profile depicts potential instability below 900 mb, while the wind profile shows two levels of vertical wind shear associated with passage through two frontal zones at 525 mb and 625 mb. The dropsonde launched at 13/0115 (not shown) also shows potential instability in the lower atmosphere and two vertical wind shear levels. The dropsonde launched at 13/0129 (Fig. 3.12), depicts frontal inversions at 900 mb and 625 mb as well as two levels of vertical wind shear at 675 mb and 825 mb. Figure 3.13 shows the13/0143z dropsonde launch, that occurred just west of the leading frontal zone. The temperature profile in this launch also shows a frontal inversion at 900 mb and only one region of vertical wind shear at 850 mb. The dropsonde data depict two sloping frontal features in the first three observations.

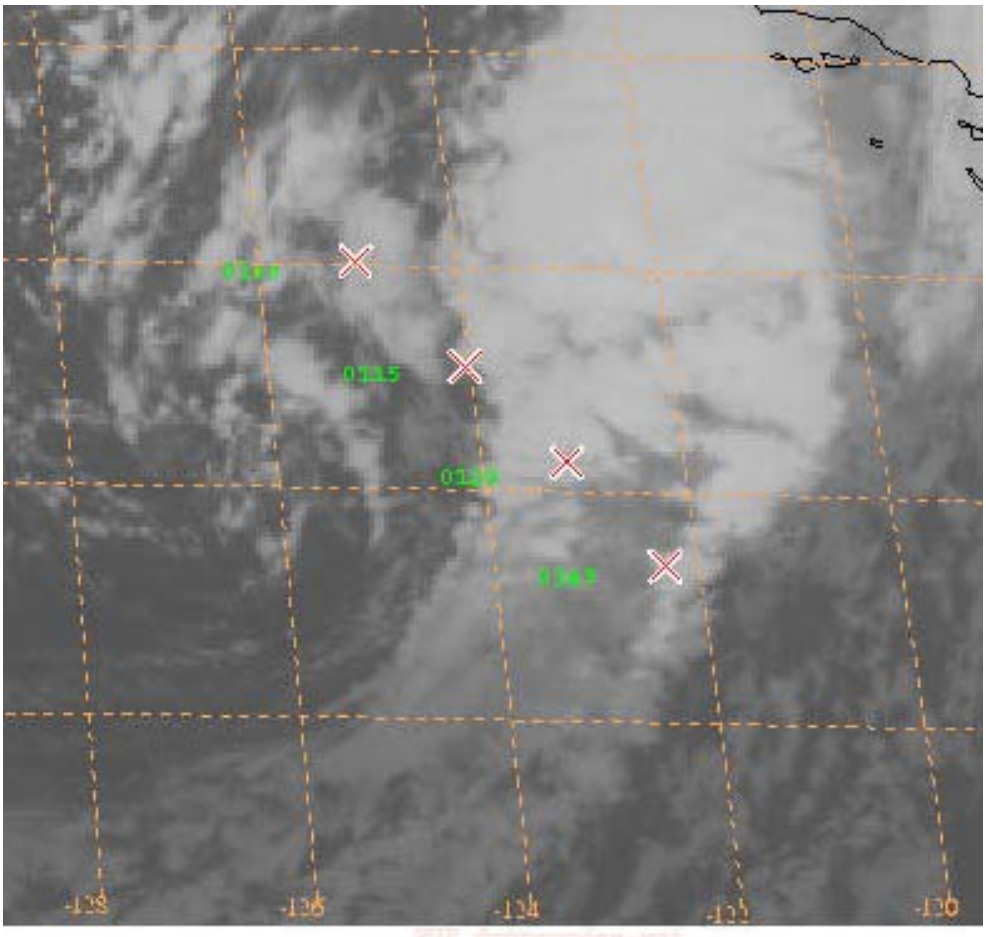

Figure 3.10. 13/01 February IR satellite imagery with the times and locations of the dropsondes plotted.

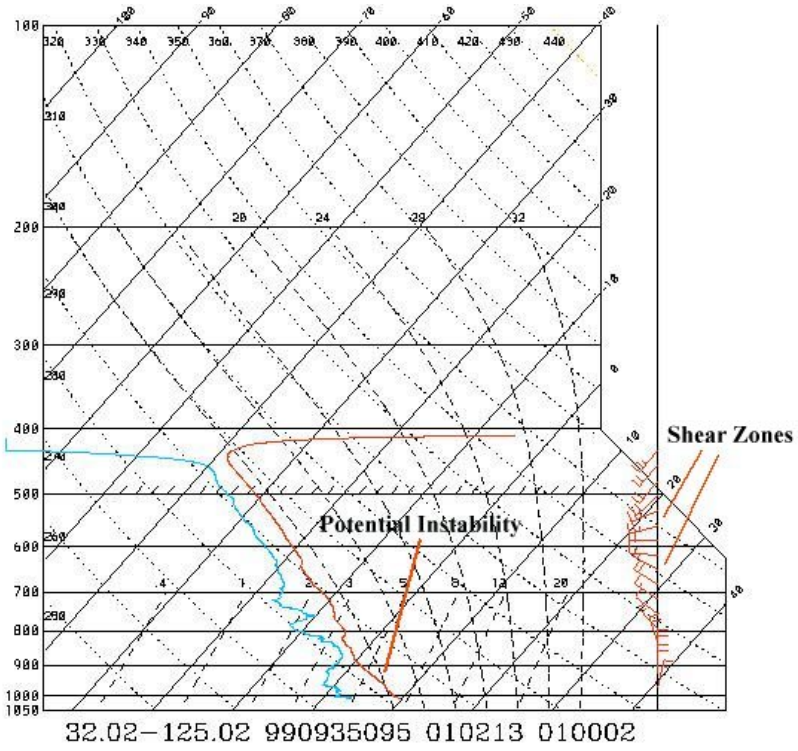

Figure 3.11. PACJET dropsonde vertical profile launched at 13/01, 32.02N 125.02W.

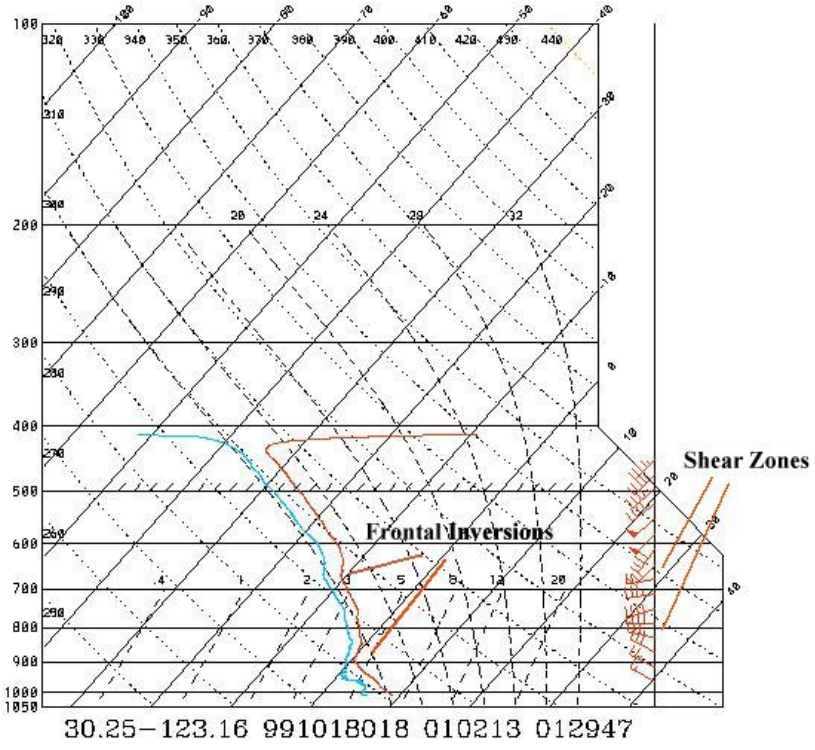

Figure 3.12. PACJET dropsonde vertical profile launched at 13/0129, 30.25N 123.16W.

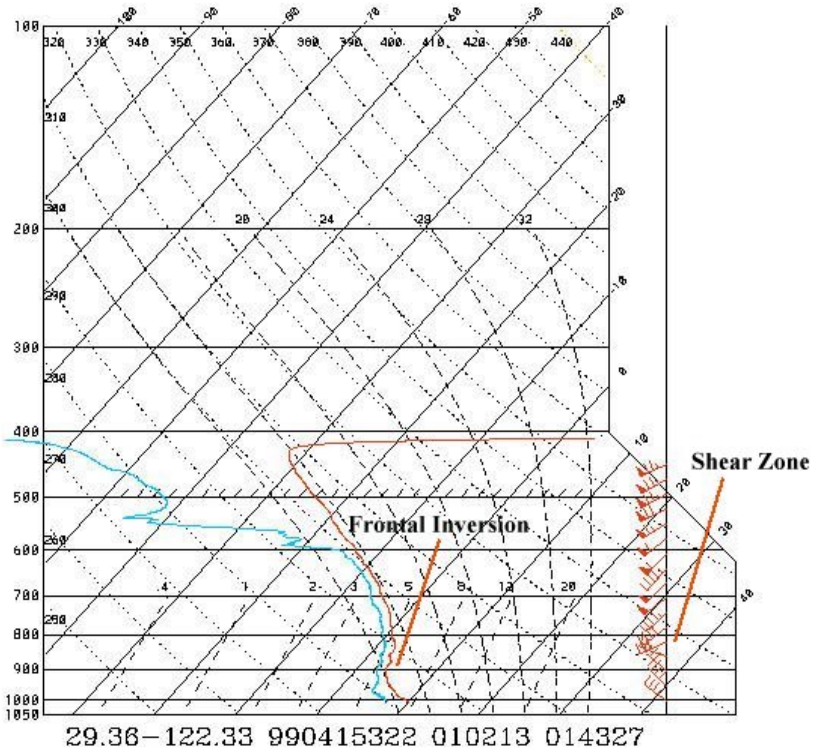

Figure 3.13. PACJET dropsonde vertical profile launched at 13/0143, 29.36N 122.33W.

Radar reflectivity data from the PACJET aircraft also supports the presence of two fronts. Figure 3.14 shows the location of the radar plot with the radar data to the right. The box is 240 km by 240 km and the lower left corner is located at 30.37N 121.66W. This is overlaid on the 13/03 IR satellite image with the positions of the lows and fronts indicated. The aircraft was transiting to the east of the storm through the leading frontal zone. The strong band of reflectivity in the center is related to this frontal feature. On the left side of the radar plot are two clusters of reflectivity corresponding to the clouds seen on the left side of the box. Unfortunately, the radar was not able to extend beyond this range to fully depict the two baroclinic zones, but it strongly supports this interpretation of the satellite imagery.

The central pressure of the primary (western) low continues to drop at the rate of 1 mb/hr throughout this period. The system tracks slowly to the east as the secondary circulation center rotates cyclonically around the main pressure center. By 13/03, stations along the southern California coast are reporting precipitation from the large cloud shield as the low moves closer to shore.

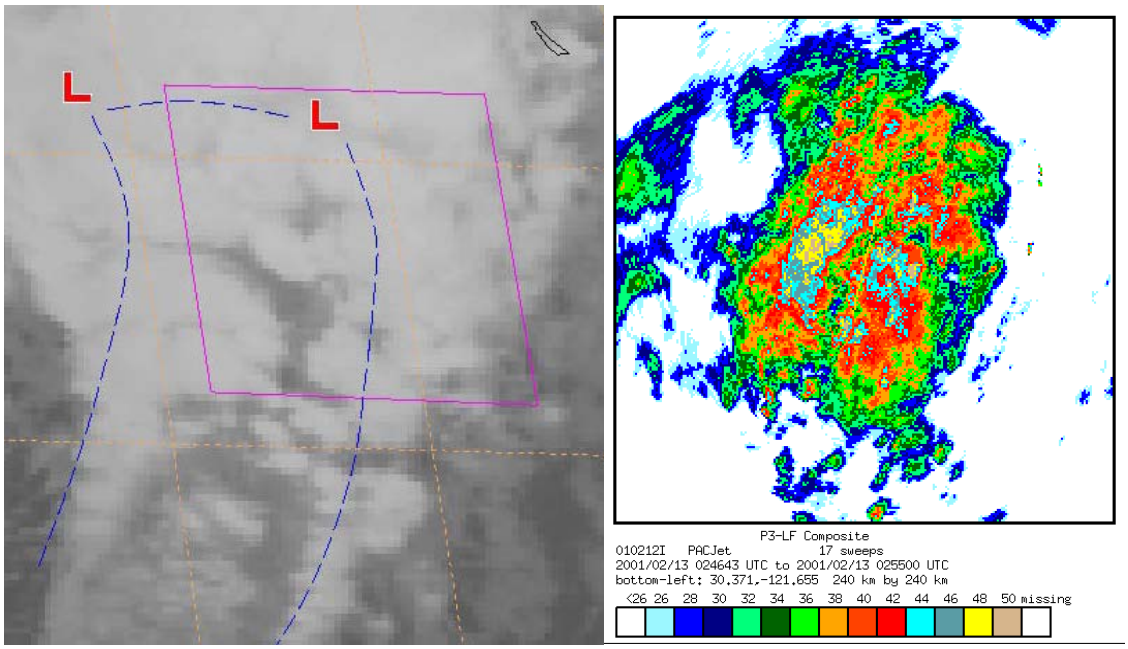

Figure 3.14. 13/03 IR satellite imagery with the location of the circulation centers and fronts plotted. The box corresponds to the radar reflectivity composite on the right taken from 13/0246z to 13/0255z.

4. Explosive Deepening Phase

a. 500 mb

Figure 3.15 shows the 13/12 IR satellite image with the COAMPS 13/12 500 mb isotach analysis and the 13/11 and 13/13 300-500 mb SATWINDS. The SATWINDS data suggests a narrow trough just off the California coast with the low downstream of the trough axis and co-located with a large area of PVA. The COAMPS analysis shows the jet streak well to the south of the low (outside of the forecast domain). SATWINDS suggest the jet streak is actually 90 nm to the north of the model position. This places the low in left exit region of the jet.

b. Surface

By 13/06, the westernmost front has begun to dissipate, however, the easternmost front is maintained and continues to move around the main pressure center along with the secondary circulation center to the east as depicted in Figure 3.16. The pressure is now 999 mb and continues to fall at 2 mb/hr through 13/09 and then approximately 1 mb/hr for the remainder of the period. By 13/08, the trailing frontal feature has completely dissipated and a dry slot becomes evident on the satellite imagery (Fig. 3.2e). The low pressure system is fully developed by 13/10, as the system now

appears as an occluded low with the secondary circulation center moving on shore. At 13/12, the system has reached its minimum pressure of 991 mb, which was well documented by a nearby buoy. After this time, the low begins to weaken and fill as it moves onshore and interacts with the land (Fig. 3.17). With the secondary low center onshore, the front now extends from it along the Southern California coast. Evident in later imagery (not shown), the secondary low appears as a triple point low to the northeast of the main low center. The system has an inverted trough associated with it that extends to the north-northwest with a closed 1004 mb isobar extending all the way to the San Francisco Bay area.

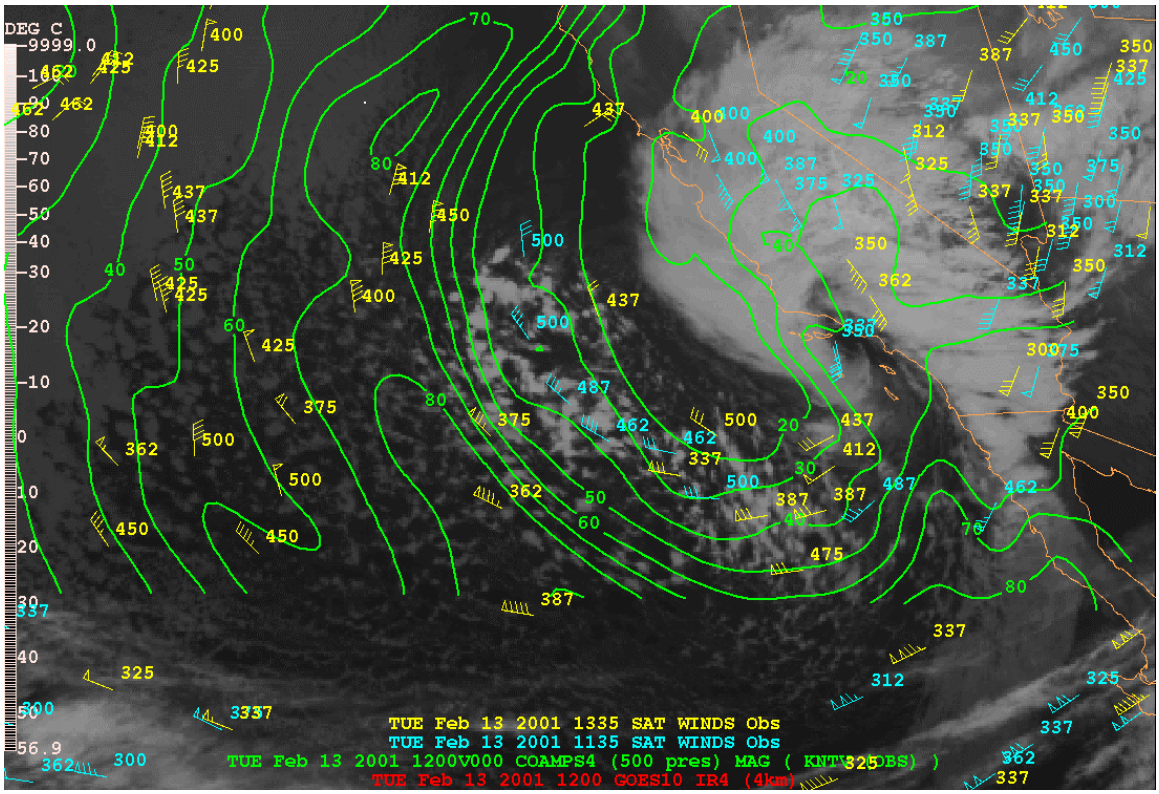

Figure 3.15. 13/12 IR satellite image with 13/12 COAMPS 500 mb isotach (kt) analysis and 300 to 500 mb SATWINDS for 13/11 (blue) and 13/13 (yellow).

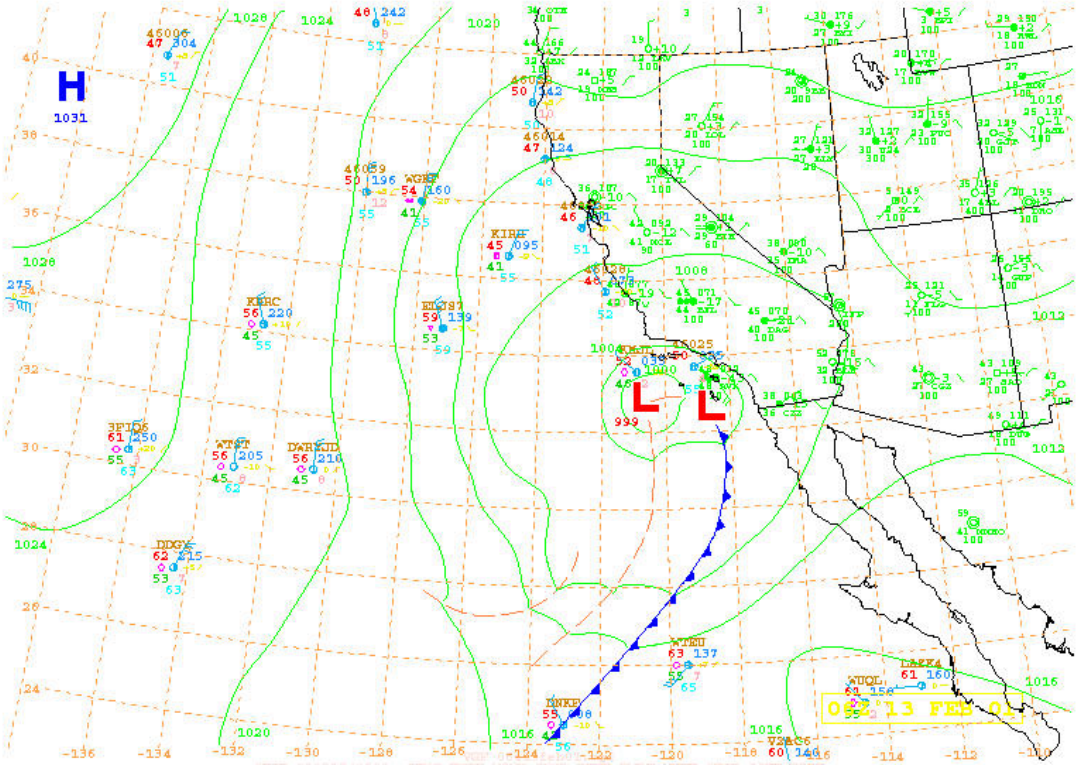

Figure 3.16. 13/06 February surface analysis with some observations plotted.

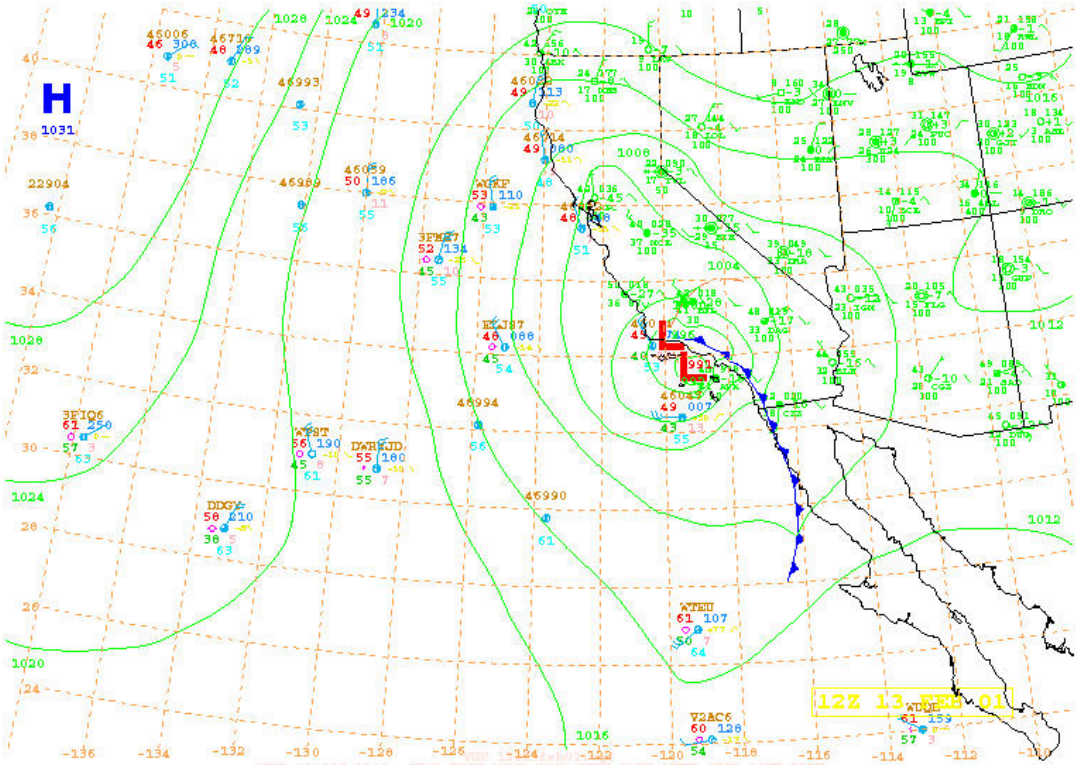

Figure 3.17. 13/12 February surface analysis with some observations plotted.

THIS PAGE INTENTIONALLY LEFT BLANK

IV. OPERATIONAL MODEL PERFORMANCE

This chapter discusses the performance of the operational models compared to the hand analysis. First the analyzed intensity and track are reviewed. Then a discussion of the model's intensity forecasts for each of the pertinent model runs are examined. This is followed by a detailing of the model's track forecasts for each of the runs. This chapter closes with an examination of possible causes for the performance of the models.

A. ACTUAL STORM INTENSITY AND TRACK

The actual evolution of the low was determined from the hand analysis discussed in Chapter III. Central pressures and positions were determined from 12/20 until 13/12, when the low reached maximum intensity. Figure 1.1 shows the sea-level pressure trend for the low and was discussed in Chapter I. For completeness in the model comparison, the National Center for Environmental Prediction (NCEP) Aviation (AVN) model and the NCEP ETA model, as well as the Navy's NOGAPS and COAMPS models, are discussed in this chapter.

Figure 4.1 shows the storm track based on the hand analysis. The plot begins at 13/00 and is then plotted at six-hour increments until 13/12. 13/00 was chosen for the first position to evaluate when the 12/12 model runs first analyzed a low for this system, even though the low first appeared at 12/20 in the hand analysis. The analyzed low starts at approximately 33N 123W and tracks to the east through 13/06. At 13/06 the low is at 33N 120.5W and begins to track to the northeast until 13/12. At 13/12, the low is positioned at 33.75N 119W.

B. FORECAST STORM INTENSITY

1. 12/12 February NWP Forecasts

The model intensity forecasts for the model runs that started at 12/12 are shown in Figure 4.2. Data points were determined by when the model plotted a low. The 13/03 forecast fields for the 12/12 run of the ETA model were missing and are therefore not plotted. NOGAPS and COAMPS did not indicate a low until the 13/12 valid time when they forecasted the low 11 mb too weak at 1002 mb. The ETA and AVN models started

forecasting the low 1009 mb, 4 mb too high and did slightly better at the 13/12 valid time with central pressures of 1001 mb and 998 mb, respectively.

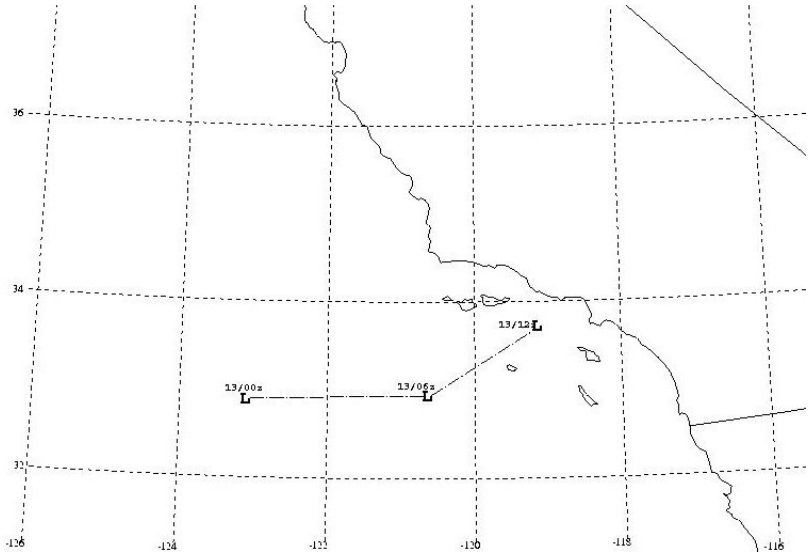

Figure 4.1. Analyzed storm track from 13/00 to 13/12 February.

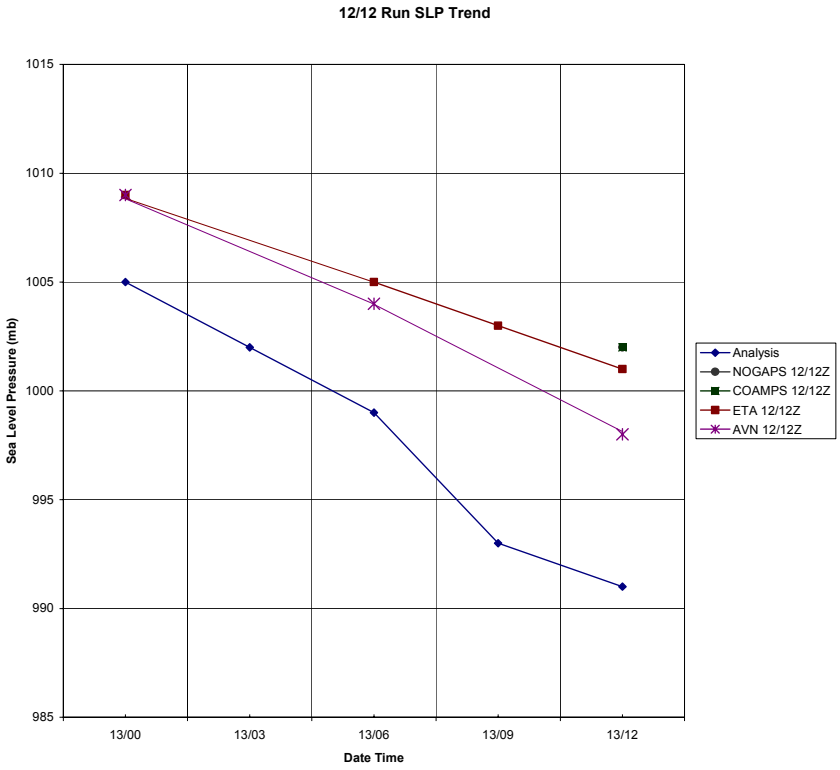

Figure 4.2. 12/12 NWP forecasts of the central pressure as compared to the analysis.

The two models, ETA and AVN, which forecasted the low from 13/00 to 13/12, however, did not capture the explosive deepening of the system. While only 1-2 mb off on the deepening rate from 13/00 to 13/06, the models maintain the same rate (AVN) for the next six hours or only slightly increase it (ETA).

2. 13/00 February NWP Forecasts

The model intensity forecasts for the model runs that started at 13/00 are shown in Figure 4.3. As with the previous model run, the central pressure was underforecast. All of the models started the forecast 4 to 5 mb too high. NOGAPS and COAMPS again resolved the storm late, not plotting a low until 13/06. With the exception of COAMPS, all the models only intensified the storm by 5 mb during the explosive phase. COAMPS, however, had the highest deepening rate at 7 mb and performed the best on the intensity forecast at 13/12, with a 997 mb central pressure. The majority of the models were within 3 mb of the COAMPS forecast. The exception was the ETA model, which produced a worse forecast than its 12/12 run forecast intensity. It started the low at 1009 mb, maintained that intensity through 13/06 and then deepened the low to 1004 mb at 13/12, 2 mb higher than its previous run.

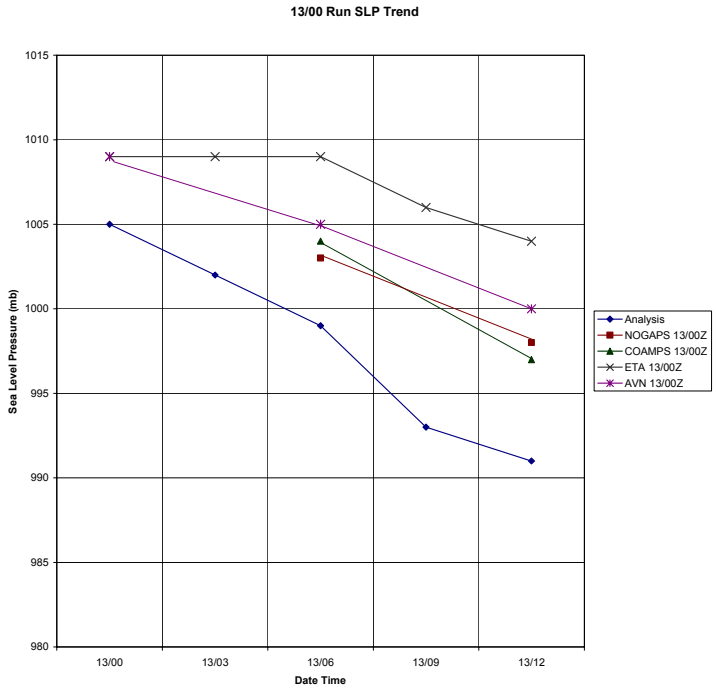

Figure 4.3. 13/00 NWP forecasts of the central pressure as compared to the analysis.

3. 13/12 February NWP Analysis

Table 4.1 shows the central pressure for the storm for the 13/12 model analysis compared to the hand analysis. The models were all at least 6 mb too high in their analysis. This occurred despite a buoy observation right at the low center reporting 991.6 mb at 13/12 and the surrounding stations reporting pressures to support a lower central pressure than depicted.

NWP Model	ANALYSIS	NOGAPS	COAMPS	AVN	ETA
SLP (mb)	991	998	998	998	997

Table 4.1. NWP central pressures for the 13/12 February analysis.

C. FORECAST STORM TRACKS

1. 12/12 February NWP Forecasts

Figure 4.4a shows the forecast tracks of the low for the 12/12 model runs. As stated above, the forecast fields for 13/03 from the 12/12 run of the ETA were missing and not plotted. The AVN model positioned the low about 120 nautical miles (nm) too far south, yet with a little greater speed of propagation its 13/12 position is in the area of the analyzed position. The ETA model positioned the low about 60 nm away and propagates the storm too slowly. Its 13/12 position is also in the area of the analyzed position. NOGAPS and COAMPS did not forecast the position of the low until the 13/12 valid time but have the location of the low close to the analyzed position. For the 13/12 forecast time (24-hr forecast), the models are all within 60 nm of the analyzed position.

2. 13/00 February NWP Forecasts

Figure 4.4b shows the forecasted tracks of the low for the 13/00 model runs. All of the models start at least 50 nm too far to the south for the 13/00 position with COAMPS the farthest away at 180 nm to the southeast. With the exception of the AVN, the 13/12 positions end up clustered around San Clemente Island, approximately 50 nm to the south of the analyzed position. The AVN 13/12 position is the closest but about 30 nm too far to the north. The ETA and AVN models tended to propagate the storm too quickly, while NOGAPS and COAMPS moved the storm too slowly.

3. 13/12 February NWP Analysis

Figure 4.4c shows the 13/12 model analysis of the low's position. Overall, the model analyses did not do too poorly, with all analyzed positions within 22 nm of the actual storm position. NOGAPS did the best and is nearly co-located with the analyzed position. The ETA and COAMPS are to the south of the analyzed position at 10 nm and 20 nm, respectively. The AVN performed the worst and is located 22 nm to the northwest of the analyzed position. These differences are most likely due to grid differences and not actual model error.

D. POSSIBLE CAUSES

To summarize, the models had several problems forecasting this storm. The models were slow to forecast the storm initially. Also, the intensity of the low was consistently weak. And the models had the cyclone tracking too far to the south in the early forecast runs.

The errors in model forecasts could be the result of a number of factors. First, the data assimilation methods used may have rejected early significant observations when compared to the first guess fields. This would explain the lateness of the models picking up this storm. Secondly, the development of this system in a data sparse area hindered the data assimilation's ability to adjust the fields to accept the storm.

Another factor is the poor handling of the upper level structure, which would have a significant impact on the development of the low in the models. The tendency of the models during this particular event, as shown in Chapter III, to blend the subpolar and subtropical jets into one jet that was not completely representative of either jet resulted in the upper level trough being overamplified. This resulted in weaker upper level support over the actual low in the models, which probably contributed to a weaker storm that was not steered correctly.

As will be shown, the models tended to mishandle the air-sea fluxes, which may have had a pronounced impact on the storm in the models. The models initially underforecast the intensity of the cold air advection over the Eastern Pacific that resulted in weaker upward fluxes than may have actually occurred. This factor will be examined in detail in Chapter V.

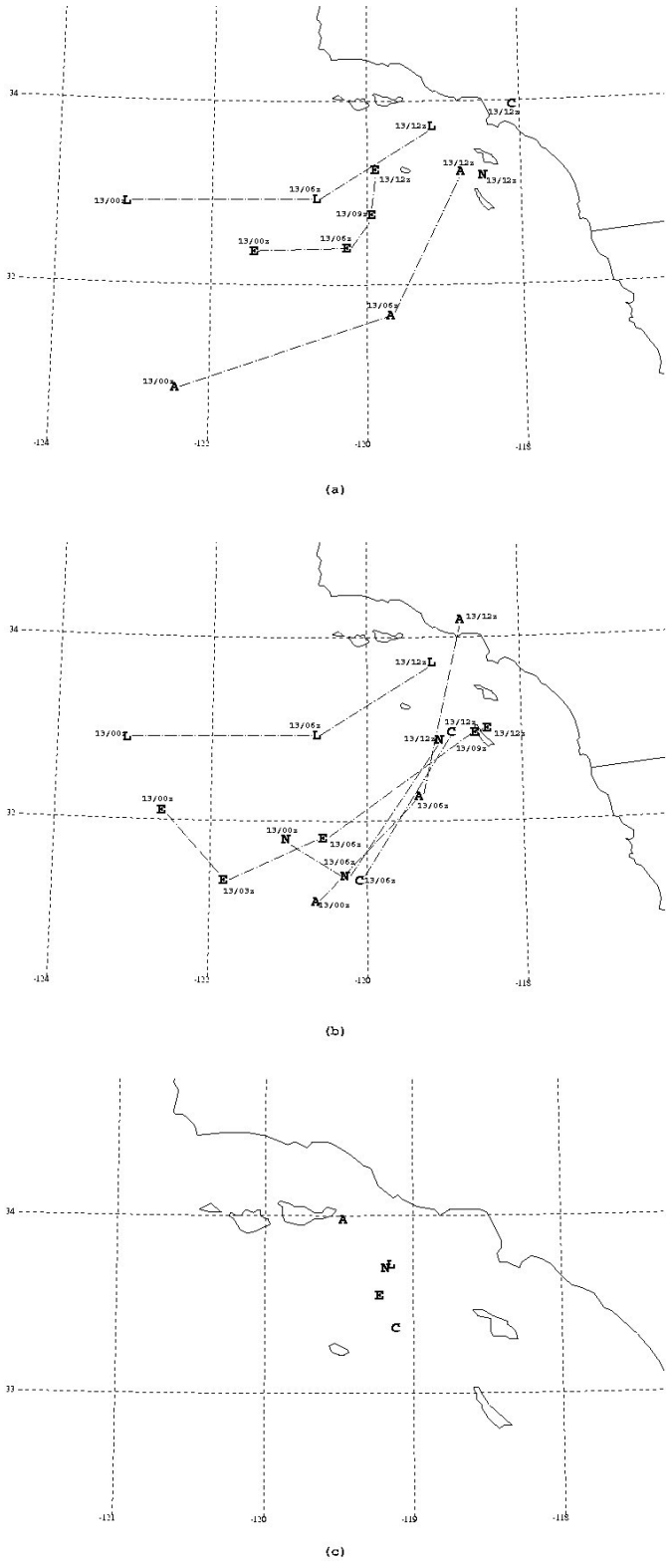

Figure 4.4. Model forecasted tracks for (a) 12/12 February model run, (b) 13/00 February model run and (c) 13/12 February model analysis: L - Analysis; N – NOGAPS; C – COAMPS; E – ETA; A – AVN.

V. AIR-SEA FLUXES

This chapter examines the possible influence of air-sea fluxes on the evolution of this cyclone. The occurrence of large upward heat and moisture fluxes in a statically unstable environment can substantially impact the cyclogenetic process when they occur near or east of the low center. To examine the potential impact of the fluxes, the model-derived fluxes and surface observations were examined. Although a complete analysis was not done, these fields provide insight into the possible impact of surface fluxes in this case.

For the purposes of determining the location of the surface heat and moisture fluxes in relation to the storm, NOGAPS sensible (heat) and latent (moisture) fluxes were plotted and compared to IR satellite imagery and ship observations. The locations of the sensible and latent heat flux maximums were then inferred from these data.

A. PRE-CYCLOGENESIS

1. Air-Sea Fluxes

In the postfrontal air mass over the Eastern Pacific, there was no strong temperature gradient present in the early time frame. The axis of stronger sensible heat fluxes from 12/00 to 12/12 shown in Figure 5.1 with arrows indicating their inferred placement given the available ship and buoy observations, produced an area of strong heating that contributes to developing a temperature gradient. The large area of organized clouds, which are clearly shown in Figure 3.2a, occurs along the axis of strongest heating. The latent heat fluxes for the same time frame (Fig. 5.2) show the axis of stronger fluxes more coincident with the cloud band than the sensible heat fluxes, suggesting that the humidity was handled reasonably well by the NOGAPS model. The inferred placements of the maximum latent heat fluxes was based on the observed air-sea temperature differences and the cloud patterns in the boundary layer. Figure 5.3 is the 12/12 IR satellite image with ship observations and the NOGAPS 12/12 2-meter air temperature (C) overlaid. The ships are reporting a negative 4 C air-sea temperature difference at this time. Just to the south of the two ship observations is the band of organized clouds (Fig. 3.2a).

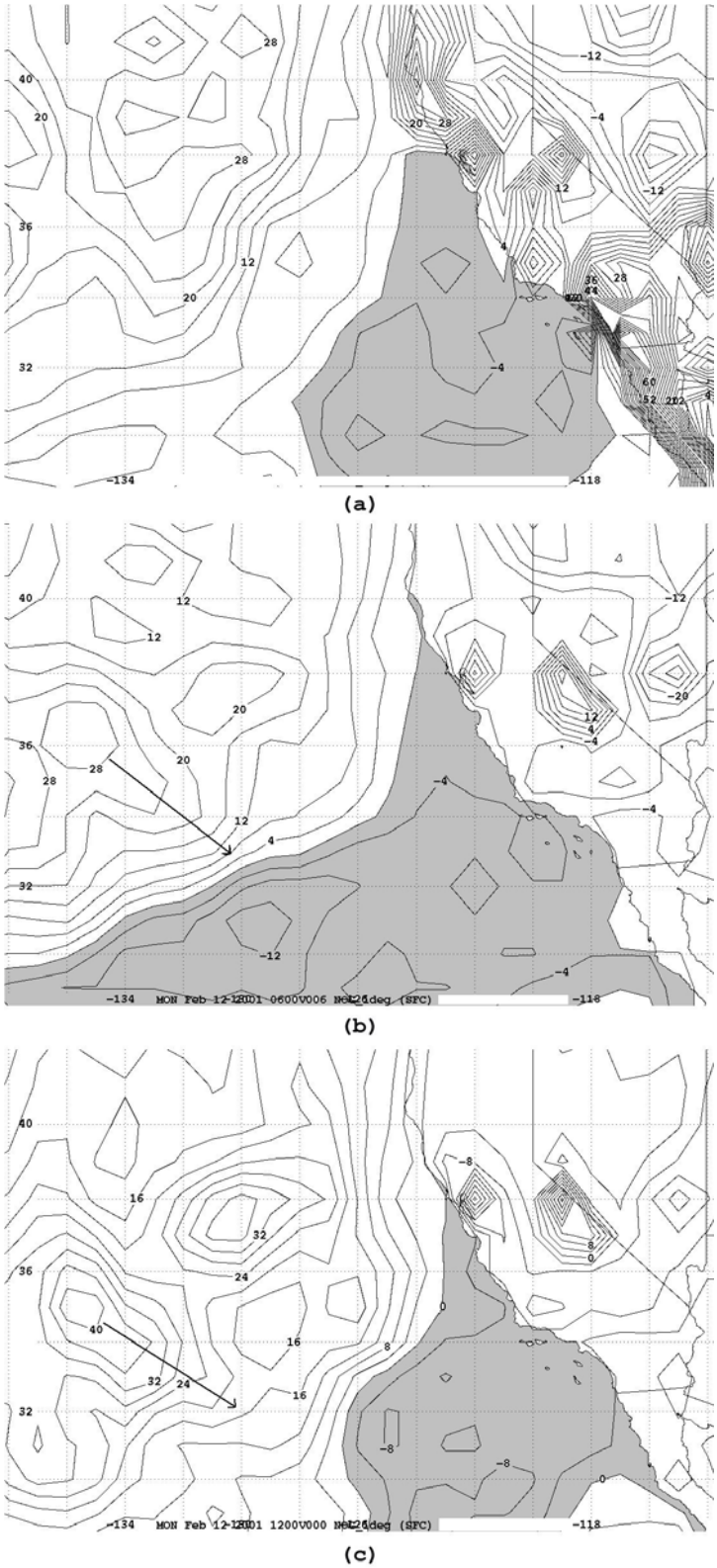

Figure 5.1. NOGAPS sensible heat fluxes (W m^{-2}) for (a) 12/00 analysis, (b) 12/06 6-hr forecast and (c) 12/12 analysis. Arrows indicated the inferred positions of the maximum fluxes.

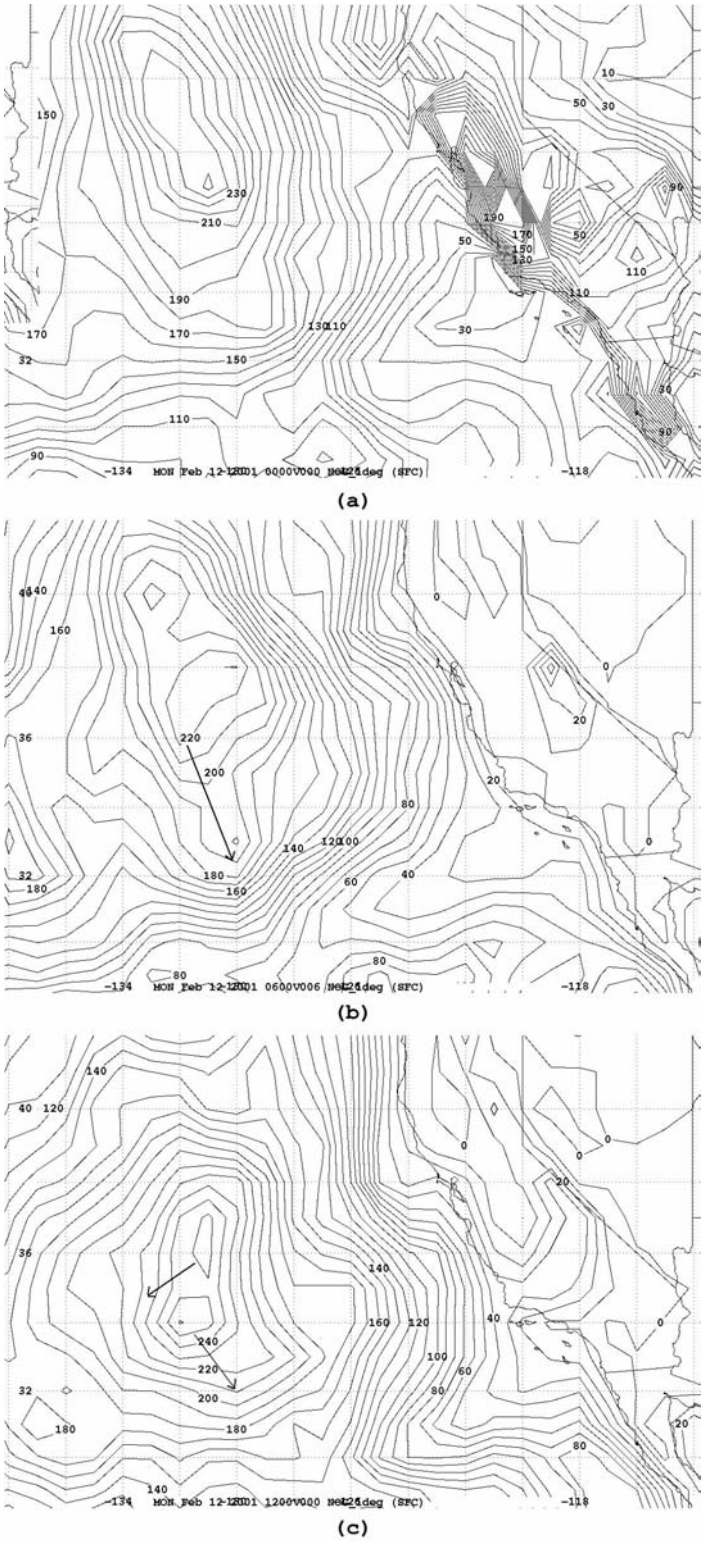

Figure 5.2. NOGAPS latent heat fluxes (W m^{-2}) for (a) 12/00 analysis, (b) 12/06 6-hr forecast and (c) 12/12 analysis. Arrows indicated the inferred positions of the maximum fluxes.

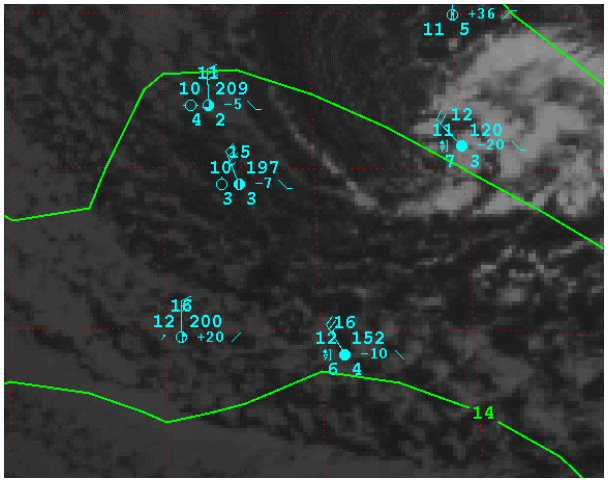

Figure 5.3. 12/12 IR satellite image with NOGAPS analyzed Air Temperature (2m) and ship reports.

In the early stages of the cyclone development, the air-sea fluxes appear to be favorably located to produce a baroclinic zone and provide moisture that interacts with the upper levels to generate a storm. With a developing baroclinic zone and the upper level support moving into a favorable position, the development of deeper vertical motion in the potentially unstable environment is likely and would contribute to cyclogenesis.

2. Static Stability

After the passage of the initial front, the air over the Eastern Pacific was potentially unstable. Figure 5.4 is a 12/0435 dropsonde launched from the PACJET aircraft at 36N 122.49W. The profile shows the low-level potential instability in the boundary layer post-frontal air below 900 mb, which if released would reach at least 500 mb. This potential instability is also readily seen in IR satellite imagery of the Eastern Pacific after the passage of a cold front, by the low-level cumulus cloud seen in Figure 5.5. Very little upward motion is required to release the potential instability that is caused by heating from the ocean surface to reach higher altitudes.

B. CYCLOGENESIS

1. Air-Sea Fluxes

The upward fluxes continue near the cyclone center through this phase of the development. Figure 5.6 shows the 13/00 IR satellite image with NOGAPS 13/00 2-meter air temperature and ship observations overlaid. The ship reports an air temperature of 11 C and a sea surface temperature of 15 C. This large air-sea temperature difference

indicates the near-surface air is being heated, which evidently feeds the convection near the low. This along with the large cloud mass with distinct convective elements is suggestive of large latent heat fluxes in the area. Figures 5.7 and 5.8 show the adjusted sensible and latent heat fluxes, respectively, during the cyclogenesis phase of the storm.

2. Static Stability

The atmosphere that the cyclone developed in continued to be potentially unstable as shown in Figure 3.10. This is evident by the large amount of clouds that occur in and around the system. The air-sea fluxes are allowed to travel to the higher atmosphere and release the associated heat and moisture in the upper atmosphere producing a large cloud shield over the system and expand the air column in the vicinity of the storm resulting in lower pressures at the surface.

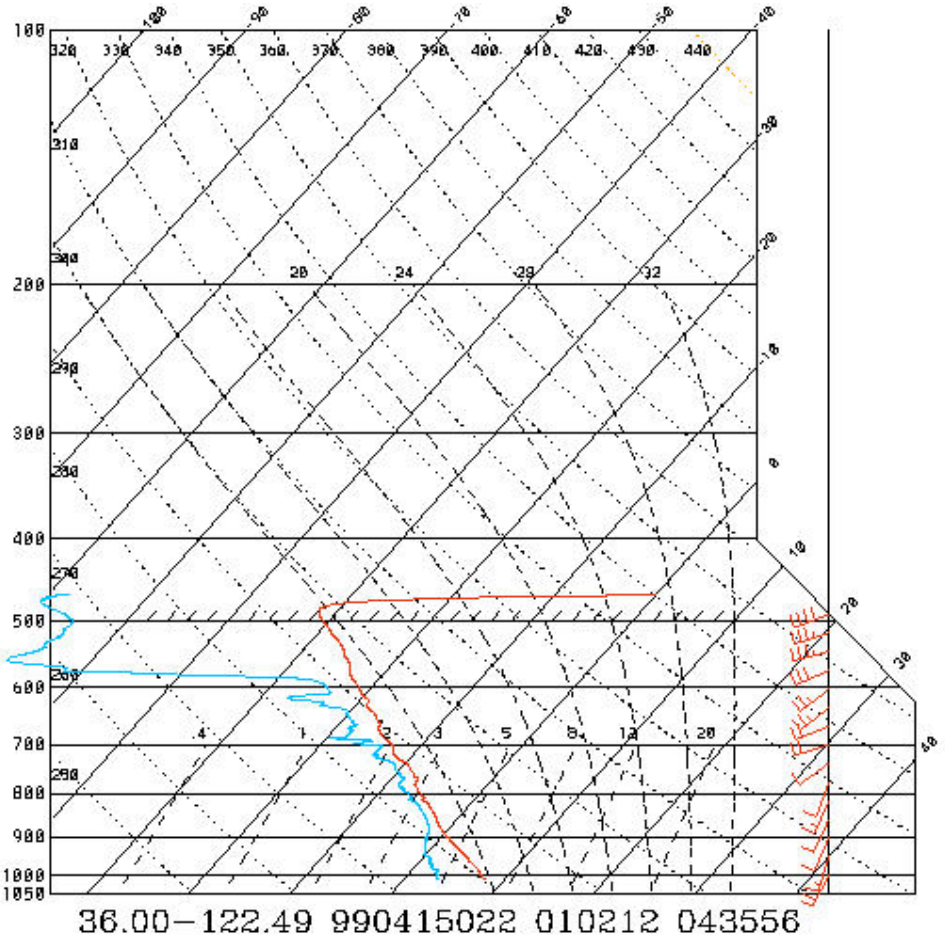

Figure 5.4. 12/0435 dropsonde launched at 36N 122.49W.

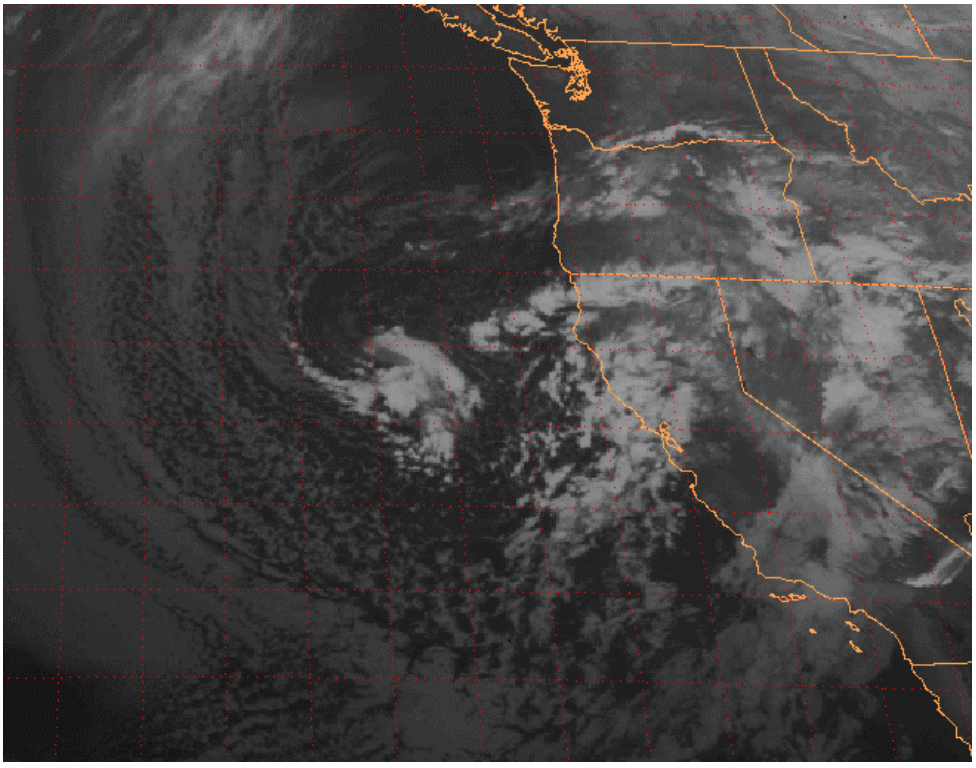

Figure 5.5. 12/06 IR satellite image showing low-level cumulus clouds associated with upward heat flux.

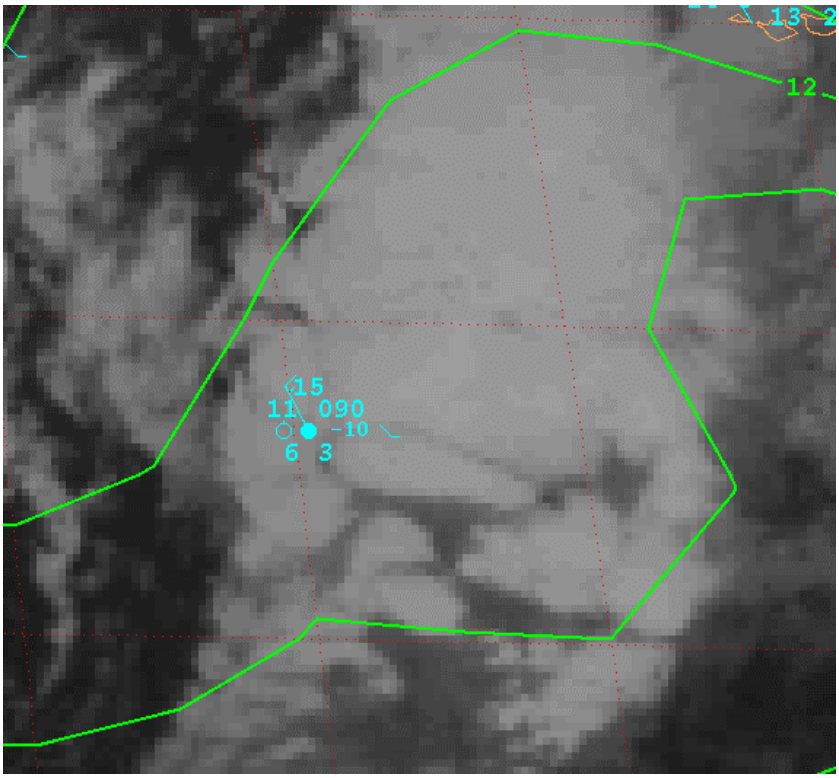

Figure 5.6. 13/00 IR satellite imagery with NOGAPS analyzed Air Temperature (2m) and ship reports.

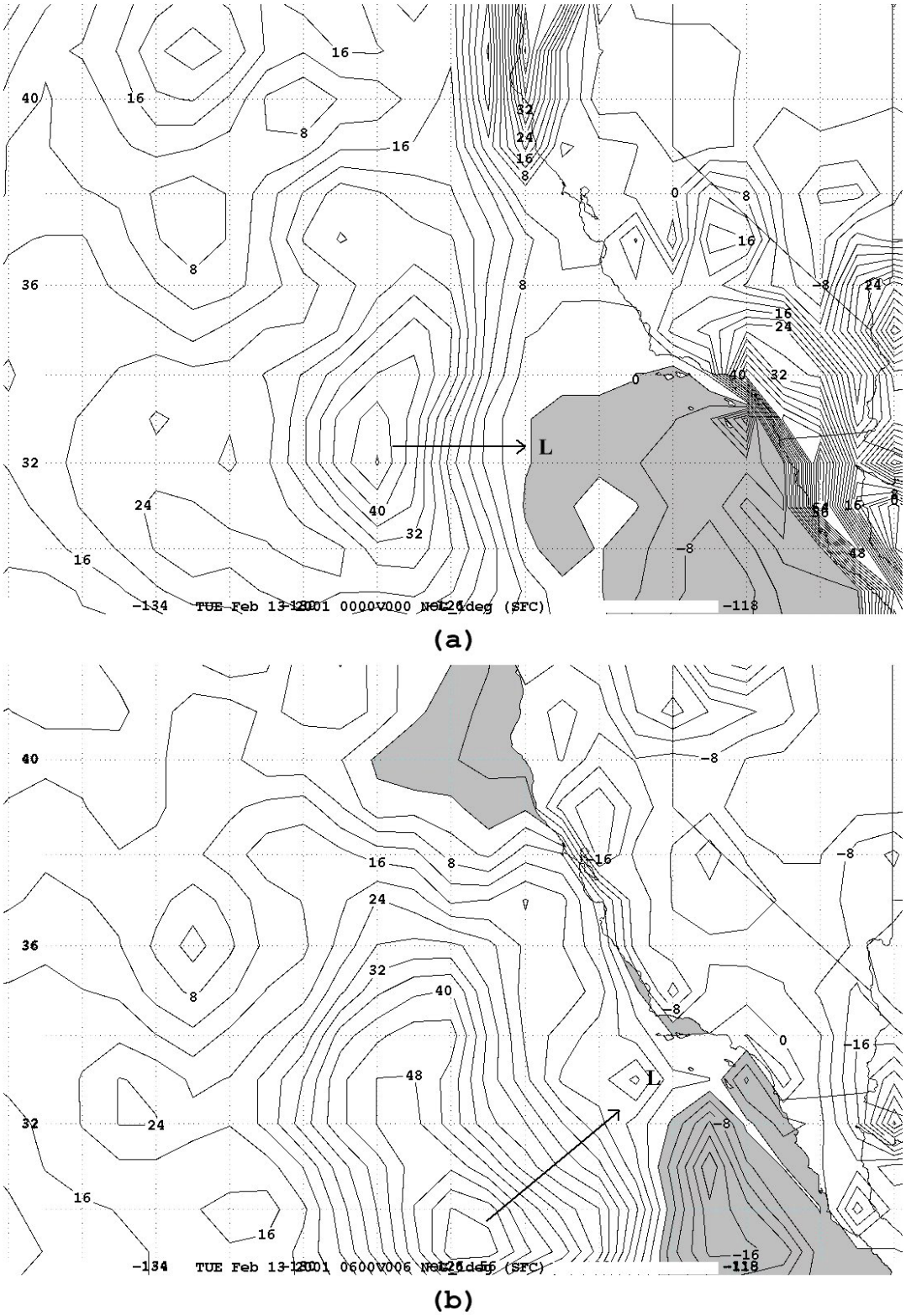

Figure 5.7. NOGAPS adjusted sensible heat fluxes (W m^{-2}) for (a) 13/00 analysis and (b) 13/06 6-hr forecast. The position of the low is indicated by the L and the inferred position of the maximum fluxes by the arrows.

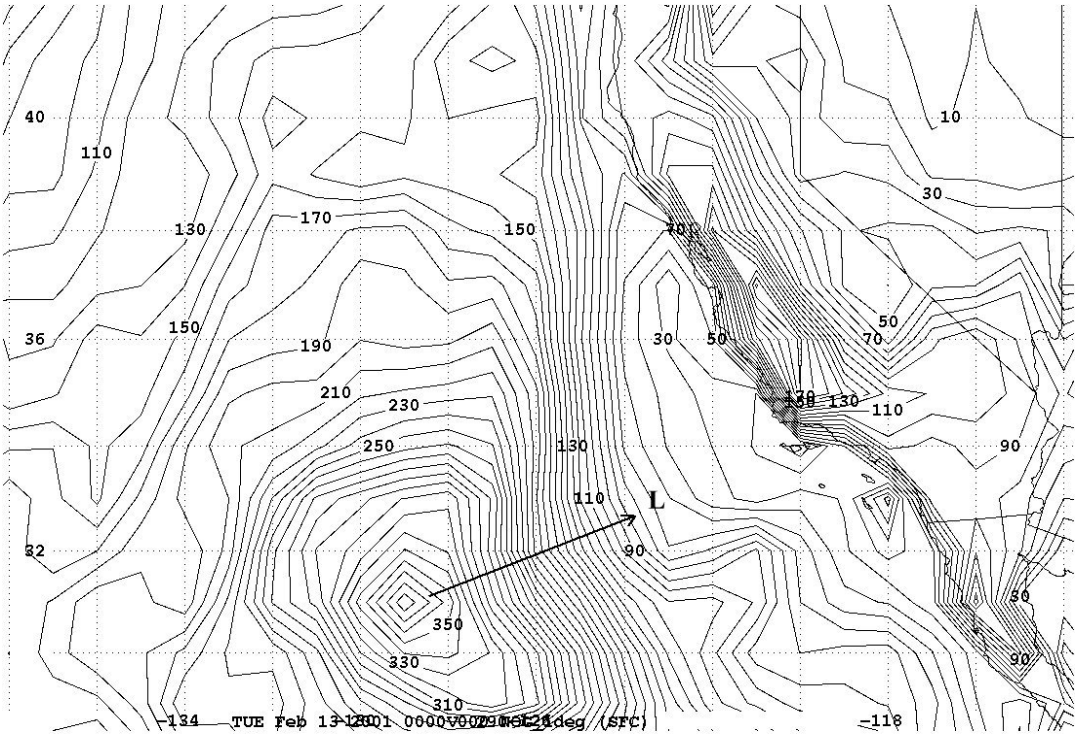

Figure 5.8. NOGAPS adjusted latent heat fluxes (W m^{-2}) for (a) 13/00 analysis (b) 13/06 6-hr forecast. The position of the low is indicated by the L and the inferred position of the maximum fluxes by the arrows.

C. EFFECTS ON THE DEVELOPMENT

The air-sea fluxes in the early stages of the development produced a region of strong surface heating and moistening in the uniform cold air mass trailing the initial front. This region of strong air-sea fluxes subsequently developed deeper convection along this region as it interacted with the upper level dynamics. Weak static stability was evidently present throughout the time period, which allowed the air-sea fluxes to destablize the environment to release the observed potential instability and enhance the cyclogenesis. It is hypothesized that this convective release of latent heat in the upper levels by the surface fluxes appears to be a key factor in the explosive cyclogenesis of this storm. Without the transport of the fluxes to the upper levels, the cyclogenesis might have been less given the lack of much of a low-level thermal gradient or baroclinic zone. This explosive cyclone appears to have developed in a manner similar to polar lows as discussed by Reed (1979).

Further evidence of the importance of the air-sea fluxes to the dynamics of this system is the almost instantaneous filling of the low as it moves on shore. As shown in Chapter III, the upper level dynamics remain favorable for the continued evolution and strengthening of the storm. However, once removed from the source of low-level heat and moisture in the air-sea fluxes, the storm degrades overland much like a tropical cyclone would. Consequently, it is reasonable to hypothesize that the air-sea fluxes were instrumental in the development of this explosive cyclone.

THIS PAGE INTENTIONALLY LEFT BLANK

VI. COMPARISON TO A SIMILAR EVENT

Reed and Albright (1986) studied a case of explosive cyclogenesis that occurred over the Eastern Pacific Ocean in November 1981. They reached a number of conclusions, which bear some similarity to this case. This chapter will contrast their conclusions to this case.

A. REED AND ALBRIGHT (1986) FINDINGS

Reed and Albright (1986) examined a storm that was an explosive cyclone that occurred in an unlikely development region in the Eastern Pacific as well. While their storm had some distinct differences, some of their findings are relevant to this case.

First, they found that their system had an unusually large and rapidly growing cloud mass. This suggested the storm was positively influenced by strong release of latent heat.

Secondly, they found that weak or neutral static stability existed in the clouds of the system and that the conditions for symmetric instability were easily met. Symmetric instability is when lines of "absolute momentum" (M-lines) transport higher values of equivalent potential temperature (θ_e) higher into the atmosphere. This allowed upward motion to easily occur in the storm system, which contributes to cyclone intensification.

Their analysis also revealed a warm core structure to the system. The cyclone had a tight inner core like a tropical cyclone, but cloud and temperature patterns of an extratropical occluded cyclone. The 1000-500 mb thickness for their case suggested a symmetrical warm core in the thermal structure.

Finally, they found that the storm track was nearly parallel to the sea surface isotherms. However, they attached no particular significance to this feature of the storm.

B. SIMILARITIES

This section discusses how this case is similar to the Reed and Albright (1986) storm. The cloud evolution, static stability structure, and surface interaction bear some resemblance to that which occurred in the Reed and Albright (1986) case.

1. Satellite Signatures

As discussed in Chapters III and V, this storm had a large and quickly growing cloud mass due to the release of latent heat in deep, organized convection. Figure 3.2 shows the growth and size of the cloud shield associated with this storm. As in the Reed and Albright case, this cyclone had a large cloud mass corresponding to the release of latent heat.

2. Symmetric Instability

Chapter V detailed the weak static stability throughout the evolution of this system, which resulted in the release of potential instability through the surface fluxes and upper-level forcing. Reed and Albright (1986) showed that their storm was characterized by weak symmetric stability, which was easily released through moistening and heating from below. The storm analyzed in the study was also susceptible to symmetric instability and more importantly absolute instability. An east-west cross section through the forecast position of the low using the COAMPS 12-hr forecast from the 13/00 run valid at 13/12 is shown in Figure 6.1. The solid lines are M-lines, while the dashed lines are θ_e. Assuming the atmosphere is saturated at this position, the figure shows absolute instability. The satellite imagery (Fig. 3.2) shows this system to be convectively active. Whether this convection is due to symmetric instability or vertical instability is not absolutely clear in the analysis done in this study. Nevertheless, the rapid, deep release of latent heat is implied by either process and would contribute to rapid cyclogenesis.

3. Warm Core Structure

Reed and Albright (1986) found a warm core structure in their case due to the release of latent heat around the tightly wound cyclone center. Without a more through analysis, a warm core structure cannot be definitively shown for this case. However, this storm had three significant similarities to the Reed and Albright (1986) storm that might suggest a warm core. First, the ability of the air-sea fluxes to reach into the upper atmosphere through deep convection near the storm center could contribute to this type of structure. Second, the rapid degeneration of the storm as it crossed the coast makes it similar to a land-falling tropical cyclone. And finally, the small tight gradient of the

system, like the Reed and Albright (1986) system, supports this possibility. These factors suggest this storm could have a warm core like the Reed and Albright (1986) storm.

4. Sea Surface Isotherms

Figure 6.2 shows the track of the storm overlaid on NOGAPS 13/00 sea surface temperature analysis. As the figure shows, the storm nearly parallels the sea surface isotherms throughout its lifespan. As in Reed and Albright (1986), the gradients are modest. Although the possible significance of this characteristic is not known, it is consistent with the prolonged upward heat and moisture fluxes that were important to the evolution of this cyclone.

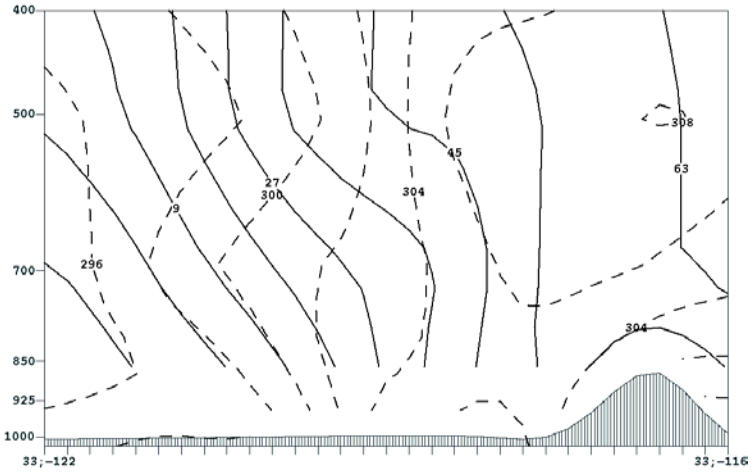

Figure 6.1. COAMPS 13/00 run 12-hr forecast, east-west cross section through the forecast position of the low showing M-lines (solid) and θ_e (dashed).

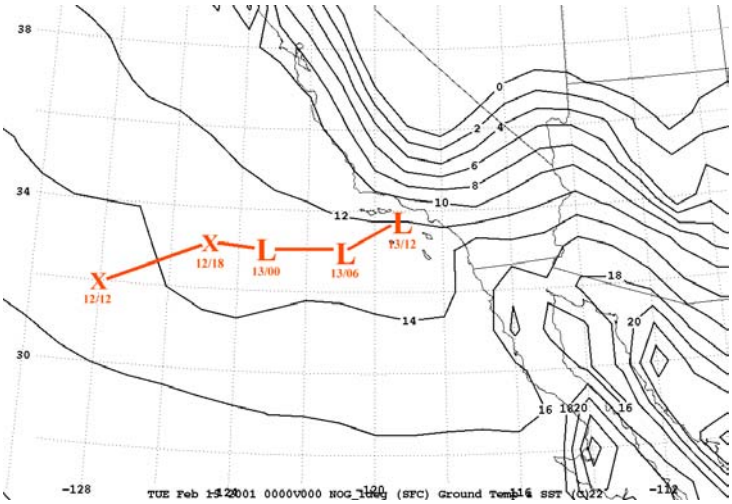

Figure 6.2. Storm track with 6-hourly positions and NOGAPS 13/00 sea surface temperatures (C).

THIS PAGE INTENTIONALLY LEFT BLANK

VII. CONCLUSIONS AND RECOMMENDATIONS

A. CONCLUSIONS

The main conclusions of this study are the following:

- The storm had double circulation centers and double baroclinic zones, which developed in cold post-frontal air.
- Due to static instability throughout the evolution of this system, air-sea fluxes contributed to deep convection and may have played a large role in the cyclogenesis of this system. The air-sea fluxes generated the cloud band and initial baroclinic zone and may have boosted the deepening of the system in the later stages through convective heat release.
- The complexity of this system coupled with the under-forecast cold air advection and blending of the upper level jet structure lead the models to poorly capture the exact track and intensity of the system. Additionally, the evolution of this cyclone in a data sparse region led the models to reject early indications of its development.
- This case was very similar to the cyclone studied by Reed and Albright (1986). These similarities suggest that this cyclone was strongly forced by convection and may have had a warm core as in the Reed and Albright (1986) case.

B. RECOMMENDATIONS

While this thesis provides a detailed description of the cyclone through its deepening phase, more detailed studies are suggested by the available data. These include:

- An examination of the timeframe beyond 13/12 is warranted to understand the mechanisms involved in the continued evolution of this complex system as it interacts with coastal topography.

- A concentrated effort to accurately depict this system using NWP is recommended. Modeling this storm correctly will greatly enhance the understanding of the dynamics involved in this interesting and complex cyclone. This effort could verify various aspects of this system including any warm core structure and the role of air-sea fluxes.
- Finally, determining the significance, if any, of the Reed and Albright (1986) storm and this storm tracking parallel to the sea surface isotherms should provide greater understanding of the role of the ocean in cyclogenesis.

LIST OF REFERENCES

Djurić, D., *Weather Analysis*, Prentice Hall, 1994.

Nuss, W.A., "Air-Sea Interaction Influences on the Structure and Intensification of an Idealized Marine Cyclone," *Monthly Weather Review*, 117, pp. 351-369, 1989.

Reed, R.J., "Cyclogenesis in Polar Air Streams," *Monthly Weather Review*, 107, pp 38-52, 1979.

Reed, R.J. and Albright, M.D., "A Case Study of Explosive Cyclogenesis in the Eastern Pacific," *Monthly Weather Review,* 114, pp. 2297-2319, 1986.

Roebber, P.J., "Statistical Analysis and Updated Climatology of Explosive Cyclones," *Monthly Weather Review,* 112, pp. 1577-1589, 1984.

Uccellini, Louis W., "Processes Contributing to the Rapid Development of Extratropical Cyclones," *Extratropical Cyclones: The Erik Palmen Memorial Volume,* pp. 81-105, American Meteorological Society, 1990.

THIS PAGE INTENTIONALLY LEFT BLANK

INITIAL DISTRIBUTION LIST

1. Defense Technical Information Center
   Ft. Belvoir, Virginia

2. Dudley Knox Library
   Naval Postgraduate School
   Monterey, California

3. Oceanographer of the Navy (N096T)
   US Naval Observatory
   Washington, District of Columbia

4. Fleet Numerical Meteorology and Oceanography Center
   Monterey, California

5. Dr. Wendell A. Nuss
   Naval Postgraduate School
   Monterey, California

6. Dr. Douglas K. Miller
   Naval Postgraduate School
   Monterey, California

7. Mr. Bob Creasey
   Naval Postgraduate School
   Monterey, California

8. F. Martin Ralph
   NOAA Environmental Technology Laboratory
   Boulder, Colorado